Organosulfates in atmospheric aerosols in Shanghai, China: seasonal and interannual variability, origin, and formation mechanisms

Yao Wang[1], Yue Zhao[1,2,*], Yuchen Wang[3], Jian-Zhen Yu[3,4], Jingyuan Shao[5], Ping Liu[1], Wenfei Zhu[1], Zhen Cheng[1], Ziyue Li[1], Naiqiang Yan[1,2], Huayun Xiao[1]

[1]School of Environmental Science and Engineering, Shanghai Jiao Tong University, Shanghai 200240, China

[2]Shanghai Institute of Pollution Control and Ecological Security, Shanghai 200092, China

[3]Division of Environment & Sustainability, Hong Kong University of Science & Technology, Hong Kong, China

[4]Department of Chemistry, Hong Kong University of Science & Technology, Hong Kong, China

[5]College of Flight Technology, Civil Aviation University of China, Tianjin 300300, China

*Corresponding author: Yue Zhao (yuezhao20@sjtu.edu.cn)

Abstract

Organosulfates (OS) are ubiquitous in the atmosphere and serve as important tracers for secondary organic aerosols (SOA). Despite intense research over years, the abundance, origin, and formation mechanisms of OS in ambient aerosols, in particular in regions with severe anthropogenic pollution, are still not well understood. In this study, we collected filter samples of ambient fine particulate matter ($PM_{2.5}$) over four seasons in both 2015/2016 and 2018/2019 at an urban site in Shanghai, China, and comprehensively characterized the OS species in these $PM_{2.5}$ samples using an ultra-performance liquid chromatography quadrupole time-of-flight mass spectrometer equipped with an electrospray ionization (ESI) source (UPLC-ESI-QToF-MS). We find that while the concentration of organic aerosol (OA) decreased by 29% in 2018/2019, compared to that in 2015/2016, mainly a result of the reduction in anthropogenic pollutant emissions in eastern China, the annually averaged concentrations of 35 quantified OS were overall similar in two years (65.5 ± 77.5 ng m^{-3}, $0.57\%\pm0.56\%$ of OA in 2015/2016 versus 59.4 ± 79.7 ng m^{-3}, $0.66\%\pm0.56\%$ of OA in 2018/2019), suggesting an increased contribution of SOA to OA in 2018/2019 than in 2015/2016. Isoprene- and monoterpene-derived OS were the two most abundant OS families, on average accounting for 36.3% and 31.0% of the quantified OS concentrations, respectively, during the two sampling years, suggesting an important contribution of biogenic emissions to the production of OS and SOA in Shanghai. The abundance of biogenic OS, particularly those arising from isoprene, exhibited strong seasonality (peaked in summer) but no significant interannual variability. In contrast, the quantified anthropogenic OS had little seasonal variability and declined in 2018/2019 compared with that in 2015/2016. The C_2/C_3 OS species that have both biogenic and anthropogenic origins averagely contributed to 19.0% of the quantified OS, with $C_2H_3O_6S^-$, $C_3H_5O_5S^-$, and $C_3H_5O_6S^-$ being the most abundant ones, together accounting for 76% of C_2/C_3 OS concentrations in 2015/2016 and 2018/2019. 2-Methyltetrol sulfate (2-MT-OS, $C_5H_{11}O_7S^-$) and monoterpene-derived $C_{10}H_{16}NO_7S^-$ were the most abundant OS and nitrooxy-OS in summer, on average contributing to 31% and 5% of the quantified OS, respectively, during the summertime of the sampling years. The substantially larger concentration ratio of 2-MT-OS to 2-methylglyceric acid sulfate (2-MA-OS, $C_4H_7O_7S^-$) in summer (6.8-7.8) than in other seasons (0.31-0.78) implies that low-NO$_x$ oxidation pathways played a dominant role in isoprene-derived SOA formation in summer, while high-NO$_x$ reaction pathways were more important in other seasons. We further find that the production of OS was largely controlled by the level of O$_x$ (O$_x$ = O$_3$ + NO$_2$), namely, the photochemistry of OS precursors, in particular in summer, though sulfate concentration, aerosol acidity, as well as aerosol liquid water content (ALWC) that could affect the heterogeneous chemistry of reactive intermediates leading to OS formation also played a role. Our study provides valuable insights into the characteristics and mechanisms of OS formation in a typical Chinese megacity and implies that mitigation of O$_x$ pollution can effectively reduce the production of OS and SOA in eastern China.

1 Introduction

Secondary organic aerosol (SOA) accounts for a significant fraction of atmospheric fine particulate matter ($PM_{2.5}$) (Jimenez et al., 2009; Huang et al., 2014) and contributes significantly to deteriorated air quality and Earth's climate forcing (Ramanathan et al., 2001; Mahowald, 2011; Shrivastava et al., 2017; Huang et al., 2014). SOA consists of thousands of organic compounds that are diverse in molecular properties. Identification and quantification of the composition of SOA are essential for understanding the composition, the chemistry of formation and evolution, properties, and climate and health impacts of SOA (Hoffmann et al., 2011; Noziere et al., 2015). However, currently only a small portion of organic matters in SOA are identified as specific compounds (Hoffmann et al., 2011; Noziere et al., 2015; Johnston and Kerecman, 2019). Organosulfates (OS) are important constituents of SOA and have been frequently detected in both polluted and clean environments (Iinuma et al., 2007a; Surratt et al., 2008; Claeys et al., 2010; Froyd et al., 2010; Hawkins et al., 2010; Hatch et al., 2011; Lin et al., 2012a; Stone et al., 2012; Hansen et al., 2014; He et al., 2014; Ma et al., 2014; Tao et al., 2014; Liao et al., 2015; Shakya and Peltier, 2015; Kourtchev et al., 2016; Meade et al., 2016; Wang et al., 2016b; Hettiyadura et al., 2017; Huang et al., 2018; Le Breton et al., 2018; Wang et al., 2018; Hettiyadura et al., 2019; Wang et al., 2019a; Brüggemann et al., 2020). It has been estimated that OS accounted for 6-12% of total sulfur in a rural area in K-puszta, Hungary (Lukacs et al., 2009), 1.3% of fine particulate organic mass (FPOM) in Fairbanks, Alaska (Shakya and Peltier, 2013), and 1-13% of FPOM across the continental United States (Tolocka and Turpin, 2012; Shakya and Peltier, 2015). Studies have also shown that OS can affect aerosol properties such as acidity, viscosity, hygroscopicity, and light-absorbing properties (Nguyen et al., 2012; Hansen et al., 2015; Estillore et al., 2016; DeRieux et al., 2018; Fleming et al., 2019; Riva et al., 2019; Olson et al., 2019).

Chamber studies have revealed that OS can originate from the (photo)oxidation of both biogenic precursors such as isoprene (Gomez-Gonzalez et al., 2008; Surratt et al., 2007b; Surratt et al., 2007a), monoterpenes (Iinuma et al., 2007a; Surratt et al., 2007a; Surratt et al., 2008; Iinuma et al., 2007b; Iinuma et al., 2009), sesquiterpenes (Chan et al., 2011), and 2-methyl-3-buten-2-ol (Zhang et al., 2012), as well as anthropogenic precursors such as polycyclic aromatic hydrocarbons, long-chain alkanes, naphthenes (Riva et al., 2015; Riva et al., 2016b), and diesel and biodiesel fuel vapors (Blair et al., 2017) in the presence of sulfate aerosol or SO_2. Many of OS observed in these chamber studies have also been detected in ambient atmosphere, among which isoprene- and monoterpene-derived OS are usually most abundant in forested, rural, and even urban areas (Stone et al., 2012; Ma et al., 2014; Meade et al., 2016; Hettiyadura et al., 2019; Kourtchev et al., 2016; Kristensen and Glasius, 2011; Wang et al., 2019a; He et al., 2014; Hatch et al., 2011; Surratt et al., 2008; Hettiyadura et al., 2017).

In addition to the precursors, detailed formation mechanisms of OS have also been widely studied (Brüggemann et al., 2020). The acid-catalyzed ring-opening reaction of epoxides was established to be an important mechanism for the formation of OS (Surratt et al., 2010; Lin et al., 2012b; Iinuma et al., 2009; Zhang et al., 2014), in particular for isoprene-derived OS (Surratt et al., 2010; Lin et al., 2012b; Hatch et al., 2011). 2-Methyltetrol sulfate (2-MT-OS, $C_5H_{11}O_7S^-$), formed via reactive uptake of isoprene epoxide (IEPOX) on sulfate, is one of the most abundant OS in atmospheric aerosol (Chan et al., 2010; Liao et al., 2015), which can contribute up to 12.6% of the organic carbon mass in Atlanta, GA (Hettiyadura et al., 2019). Another OS formation pathway is the nucleophilic substitution of tertiary organonitrates by inorganic sulfate. Darer et al. (2011) found that tertiary organonitrates are thermodynamically unstable and can undergo nucleophilic substitution with sulfate to generate

79 OS rapidly. This mechanism can also explain the formation of some nitrooxy-OS (NOS). In atmospheric aqueous phase,

80 sulfate radicals that can be produced by oxidation of S(IV) species in the presence of transition metal ions (TMI) (Grgic et al.,

81 1998; Herrmann, 2003) or by OH radical reaction with bisulfate (Herrmann, 2003; Jiang et al., 1992) can also react with

82 unsaturated organic compounds to form OS. Laboratory studies have shown that a large number of OS were produced by the

83 bulk aqueous-phase oxidation of aromatic compounds, isoprene or its oxidation products, methyl vinyl ketone (MVK) and

84 methacrolein (MACR), in the presence of inorganic sulfate or peroxodisulfate under irradiation (Nozière et al., 2010;

85 Schindelka et al., 2013; Huang et al., 2020), or in the presence of S(IV) and TMI under dark conditions (Huang et al., 2019).

86 However, field observational evidence for this mechanism is still lacking. In addition, reactive uptake of SO_2 on organic

87 aerosol can also result in the production of OS. Laboratory studies have found that sulfur dioxide (SO_2) could react with C=C

88 bond in unsaturated fatty acids under dark conditions to form OS (Shang et al., 2016). Such OS have been detected in ambient

89 atmosphere with an estimated contribution of 0.3‰-0.9‰ to OM in $PM_{2.5}$ in southern China (Zhu et al., 2019). Recent studies

90 have also shown efficient production of OS from heterogeneous/aqueous-phase reactions of SO_2 with organic peroxide-

91 containing aerosol and SOA (Wang et al., 2019b; Yao et al., 2019). Such OS production was found to be mainly a result of

92 the direct reaction between SO_2 and peroxides, rather than acid-catalyzed reaction involving inorganic sulfate (Wang et al.,

93 2019b). Currently, the acid-catalyzed ring-opening reaction of IEPOX has been the most well-studied mechanism and proved

94 to be important in atmospheric OS formation by both field and modelling studies (Surratt et al., 2010; Kourtchev et al., 2016;

95 Hettiyadura et al., 2019; Hatch et al., 2011; Chan et al., 2010; McNeill et al., 2012; Worton et al., 2013; He et al., 2018; Pye

96 et al., 2013). However, atmospheric importance of other OS formation mechanisms remains to be evaluated.

97 The OS formation pathways aforementioned can be affected by aerosol properties such as acidity, aerosol liquid water content

98 (ALWC), and sulfate concentration. There is ample evidence from laboratory studies that increased aerosol acidity

99 significantly enhances the production of OS from acid-catalyzed reactions (Iinuma et al., 2007b; Chan et al., 2011; Surratt et

100 al., 2007a; Surratt et al., 2007b; Zhang et al., 2012), while field studies have shown that the abundance of OS was not or only

101 weakly correlated with aerosol acidity in some locations (Nguyen et al., 2014; Budisulistiorini et al., 2015; Brüggemann et

102 al., 2017; Rattanavaraha et al., 2017), suggesting the existence of other factors (e.g., ALWC, sulfate content, etc.) that control

103 OS formation in these areas. ALWC has dual effects on OS formation. On one hand, elevated ALWC can reduce the viscosity

104 and/or inhibit the liquid-liquid phase separation of aerosol, which would favor the dissolution and mixing of reactive

105 intermediates such as IEPOX and multifunctional aldehydes in aqueous sulfate aerosol (Shiraiwa et al., 2011; Liao et al., 2015;

106 McNeill et al., 2012) or SO_2 in organic aerosol (Shang et al., 2016; Passananti et al., 2016; Yao et al., 2019), thereby enhancing

107 OS formation. On the other hand, high ALWC would decrease aerosol acidity via dilution, hence inhibiting the acid-catalyzed

108 OS formation. High ALWC may also promote the hydrolysis of OS in aqueous aerosol (Darer et al., 2011).

109 Quantification of OS is important for understanding their abundance and the chemistry of formation and evolution in the

110 atmosphere. Owing to the lack of authentic standards, the quantification of OS remains a challenging task. Recently, several

111 research groups have synthesized a series of authentic standards (e.g., glycolic acid sulfate, lactic acid sulfate, hydroxyacetone

112 sulfate, 2-methyltetrol sulfate, benzyl sulfate, α-pinene sulfate, β-pinene sulfate, and limonene sulfate) that are structurally

113 the same or similar with the OS found in atmospheric aerosols (Kundu et al., 2013; Staudt et al., 2014; Hettiyadura et al.,

114 2015; Wang et al., 2017; Olson et al., 2011; Huang et al., 2018; Budisulistiorini et al., 2015). They used these authentic

standards to quantify OS in ambient aerosols and provided important constraints on the abundance, origin, and chemistry of OS in the atmosphere.

Up to date, there are few studies characterizing atmospheric OS in areas with severe anthropogenic pollution. Situated in the eastern Yangtze River Delta (YRD) of China, Shanghai has a population of more than 24 million and is plagued by air pollution (Behera et al., 2015; Wang et al., 2016a). Here we conducted a comprehensive investigation of the molecular composition, abundance, sources, and formation processes of OS in ambient aerosols in Shanghai. More than 150 ambient $PM_{2.5}$ samples collected over four seasons during both 2015/2016 and 2018/2019 in urban Shanghai were analyzed using UPLC-ESI-QToF-MS, and 35 OS were quantified using 7 synthesized and commercially purchased OS standards. Seasonal and interannual variations of OS, in response to the changes in emissions, meteorological conditions, and $PM_{2.5}$ chemical compositions, were comprehensively characterized, and the influencing factors such as aerosol acidity, ALWC, sulfate content, oxidant level and so on for OS formation were probed. This study would help to understand the characteristics and mechanisms of OS and SOA production under the strong influence of anthropogenic pollution in Chinese megacities.

2 Materials and methods

2.1 Ambient Sample collection

In total 156 ambient $PM_{2.5}$ samples were collected from 8 April 2015 to 16 January 2016 and from 23 October 2018 to 5 August 2019 in Shanghai, China. The sampling site is located on the rooftop of a 20-meter-tall teaching building on the Xuhui Campus of Shanghai Jiao Tong University at 31.201°N, 121.429°E, which is in downtown and surrounded by residential and commercial areas (see Fig. 1a, b). There is a main street 230 m east to the sampling site. The $PM_{2.5}$ samples were collected on pre-baked (550 °C, 8 h) quartz-fiber filters (Whatman) from 9:00 am to 8:00 am of the next day using a high-volume sampler (HiVol 3000, Ecotech) at a flow rate of 67.8 m^3 h^{-1}. The collected samples were wrapped in pre-baked (550 °C, 8 h) aluminum foil and stored at -20 °C before analysis.

2.2 Organosulfate measurement with UPLC-ESI-ToF-MS

An aliquot of ~17 cm^2 was removed from each filter sample and extracted in 3 mL of methanol (LC-MS grade, CNW Technologies GmbH) twice under sonication in an ice bath at 4 °C for 30 min. The extracts derived each time were combined and filtered through a 0.45 μm poly tetra fluoroethylene (PTFE) syringe filter (CNW Technologies GmbH) to remove insoluble materials, and subsequently concentrated to 250 μL with a gentle stream of ultra-high-purity nitrogen (Shanghai Likang Gas Co., Ltd). The resulting extracts were mixed with ultrapure water (milliQ, 18.2 MΩ·cm) of the same volume and centrifugated at 12000 rpm and 4 °C for 20 min using a centrifuge (Cence, TGL-16M) to get supernatant for analysis.

The resulting solutions were analyzed using an Acquity UPLC (Waters) coupled to a Xevo G2-XS QToF-MS (Waters) having a mass resolving power of ≥ 40000 and equipped with an ESI source. The analytes were separated by an ethylene bridged hybrid (BEH) C_{18} column (2.1×100 mm, 1.7 μm particle size, waters) at 50 °C. A gradient elution procedure was performed using water (A) and methanol (B) both containing 0.1% acetic acid (v/v) as the eluents: A was maintained at 99% for 1.5 min, decreased to 46% in 6.5 min and to 5% in 3 min, then decreased to 1% in 1 min and held for 2 min, finally returned to 99% in 0.5 min and held for 1.5 min to equilibrate the column. The total eluent flow rate was 0.33 mL min^{-1} and the sample injection

149 volume was 2.0 µL. The ESI source was operated in the negative ion mode under optimum conditions as follows: capillary

150 voltage 2.0 kV, sampling cone voltage 40 V, source offset voltage 80 V, source temperature 115°C, desolvation gas temperature

151 450°C, cone gas 50 L h^{-1}, desolvation gas 900 L h^{-1}.

152 The quantified OS as well as the authentic and surrogate standards used for the quantification of each OS are listed in Table

153 1. The OS standards were selected by mainly referring to Hettiyadura et al. (2019), which is based upon a comparison of the

154 MS/MS pattern between authentic standards and targeted OS in ambient aerosols, as well as to Wang et al (2018). Glycolic

155 acid sulfate (GAS, $C_2H_3O_6S^-$) and lactic acid sulfate (LAS, $C_3H_5O_6S^-$) were synthesized according to Olson et al. (2011).

156 Because LAS and GAS are too small in molecular size, we could not find a promising stain and use thin layer chromatography

157 (TLC) on silica gel to purify them. Instead, we employed ^{1}H NMR and an internal standard (dichloroacetic acid) to determine

158 their purities (8% for GAS and 15% for LAS). Limonaketone sulfate ($C_9H_{15}O_6S^-$) and α-pinene sulfate ($C_{10}H_{17}O_5S^-$)were

159 synthesized and details were described in Wang et al. (2017). Other OS standards including sodium methyl sulfate ($CH_3O_4S^-$,

160 99%, Macklin), sodium octyl sulfate ($C_8H_{17}O_4S^-$, 95%, Sigma-Aldrich), and potassium phenyl sulfate ($C_6H_5O_4S^-$, 98%, Tokyo

161 Chemical Industry, Shanghai) were commercially purchased. The quantified OS were also analyzed in tandem mass

162 spectrometry (MS/MS) at a collision energy of 10-50 eV to confirm whether they are OS by sulfur-containing fragment ions

163 observed. In this study, most quantified OS were fragmented to the bisulfate anion (m/z 97) and several quantified OS were

164 only fragmented to the sulfate radical anion (m/z 96) and the sulfite radical anion (m/z 80) (see Fig. S1).

165 **2.3 Auxiliary measurements**

166 Meteorological parameters, including temperature, relative humidity (RH), and wind speed (WS) were continuously

167 monitored by Shanghai Hongqiao international airport station, which is 9 km west to the sampling site (Fig. 1c). The

168 concentrations of SO_2, nitrogen dioxide (NO_2), O_3 and $PM_{2.5}$ were measured by a state-controlled air quality monitoring

169 station on the Xuhui Campus of Shanghai Normal University, which is 4.5 km southwest to the sampling site for the $PM_{2.5}$

170 filter samples (Fig. 1c). Organic carbon (OC) and elemental carbon (EC) in $PM_{2.5}$ filter samples were measured by a thermal-

171 optical multiwavelength carbon analyzer (DRI Model 2015). The concentration of OM was derived by multiplying the OC

172 by 1.6 (Tao et al., 2017). Water-soluble inorganic compounds including sulfate, nitrate, chloride, ammonium, potassium, and

173 calcium were analyzed with an ion chromatograph (Metrohm MIC). The seasonal and annual average values of meteorological

174 parameters and concentrations of trace gases, $PM_{2.5}$ and its major components in 2015/2016 and 2018/2019 are listed in Table S1.

175 **2.4 Estimation of aerosol liquid water content and pH**

176 The ISORROPIA-II thermodynamic model (Fountoukis and Nenes, 2007) was employed to predict ALWC and aerosol pH.

177 The aerosol water-soluble inorganic ion concentrations, as well as temperature and RH were used as the model input. The

178 model was run in the forward model for metastable aerosol, which was shown to give a more accurate representation of

179 aerosol pH than using the reverse-mode calculations when with only aerosol data input (Guo et al., 2015; Hennigan et al.,

180 2015). ISORROPIA-II calculates the equilibrium concentration of aerosol hydronium ions (H^+_{air}) per volume of air (µg m^{-3}),

181 along with ALWC (µg m^{-3}). The aerosol pH was then derived by

$$\text{pH} = -\log_{10}(\text{H}^+_\text{aq}) = -\log_{10}\frac{1000\text{H}^+_\text{air}}{\text{ALWC}}, \qquad (1)$$

where H^+_aq is the concentration of hydronium ions in aqueous aerosol (mol L^{-1}). In this study, ALWC associated with organic aerosol and its influences on aerosol pH were not considered. However, previous studies showed that water uptake by organic aerosol only contributed to a minor fraction (5%) of total ALWC and had a negligible influence on aerosol pH in haze events in China (Liu et al., 2017). The seasonally and annually averaged ALWC and aerosol pH levels in 2015/2016 and 2018/2019 are also given in Table S1.

2.5 Quality control

The extraction efficiency of OS species in filter samples was evaluated by measuring the recovery of ten different OS standards (see Table S2). The synthesized and commercially purchased OS standards were spiked into blank and pre-baked quartz filters, followed by extraction and analysis with the same procedures for ambient samples. The recoveries of OS standards were about 84-94% except for Δ-Carene OS, Lactic acid sulfate, and Glycolic acid sulfate, the recovery of which was 66%, 72.5%, and 77.8%, respectively (see Table S2). This result suggests a fairly high extraction efficiency for the majority of OS species in this study.

In addition, we evaluated the matrix effect on the signal response of OS by comparing the measured signal intensity of OS standards added to the extracts of ambient PM$_{2.5}$ filter samples with that of pure OS standard solutions. Table S3 gives the ratios of measured signal intensity of OS standards in filter sample extracts to that in pure solutions. As for the standards that were already present in the samples, we subtracted the response in the sample from the total (sample + standard) before calculating the ratio. Most of OS standards had a ratio around 1, suggesting no obvious matrix effect on the measurement of the majority of OS species. However, the two smallest OS standards, methyl sulfate and glycolic acid sulfate that were the very first species eluted from LC column, had a ratio significantly smaller than 1, suggesting the inhibited ionization of these two OS likely by the highly soluble and polar species in the filter samples that were co-eluted with these two OS. We note that the matrix effect for these two OS is dependent on the PM$_{2.5}$ mass loading. For example, the signal ratio of glycolic acid sulfate standard measured in filter sample extracts versus in pure solutions ranged from 0.17-0.31 (Exps. 1-2) for very polluted days to 0.45-0.53 for clean days (Exps. 3-4). This implies that the abundance of glycolic acid sulfate in ambient aerosols reported here may be underestimated by a factor of 2-6 due to the matrix effect.

3 Results and Discussion

3.1 Overview of pollution characteristics during sampling periods

Figure 2 shows the time series of meteorological parameters, O$_3$, NO$_2$, SO$_2$, PM$_{2.5}$ and its major components, as well as H^+_aq and ALWC during the sampling periods. The average values (concentrations) of each parameter (species) were given in Table S1. The meteorological conditions (wind speed, temperature, and RH) were overall similar in 2015/2016 and 2018/2019. While the NO$_2$ concentration decreased from 27.0±13.0 ppb in 2015/2016 to 21.3±10.3 ppb in 2018/2019, the O$_3$ level had no obvious difference in two years (29.8±15.2 ppb in 2015/2016 versus 29.6±13.9 ppb in 2018/2019), consistent with the

214 nonlinear response of O_3 production to precursor emissions (Liu and Wang, 2020). The annual average mass loading of $PM_{2.5}$

215 declined by 34.5% in 2018/2019 (38.6 ± 24.0 μg m^{-3}) compared to that 2015/2016 (59.0 ± 37.9 μg m^{-3}), largely driven by the

216 strong decrease in the abundance of OM (29.1%) and sulfate (37.4%). The decrease of $PM_{2.5}$, OM, and sulfate concentrations

217 from 2015/2016 to 2018/2019 reflects a significant reduction in anthropogenic pollutant emissions in eastern China in recent

218 years. In contrast to OM and sulfate, the concentration of nitrate had little change between 2015/2016 (8.8 ± 8.9 μg m^{-3}) and

219 2018/2019 (8.4 ± 7.8 μg m^{-3}), despite an obvious decrease in NO_2 concentration. This is at least partly a result of reduced

220 aerosol acidity (H^+_{aq}, see Fig. 2 and Table S1) and thereby enhanced partitioning of HNO_3 into the particle phase. Furthermore,

221 the nitrate concentration showed a strong seasonality, ranging from 1.0 ± 1.1 and 3.4 ± 3.2 μg m^{-3} in summer to 16.6 ± 10.0 and

222 14.1 ± 10.0 μg m^{-3} in winter in 2015/2016 and 2018/2019, respectively, partly owing to the seasonal variation of temperature

223 and aerosol acidity that modulates the gas/particle partitioning of nitrate (Fisseha et al., 2006; Guo et al., 2015; Griffith et al.,

224 2015; Guo et al., 2016). A similar strong reduction in $PM_{2.5}$ concentration and variations in aerosol composition over the past

225 several years were observed in different regions in China (Tao et al., 2017; Wang et al., 2020b; Ding et al., 2019a; Wen et al.,

226 2018). As a result of strong reductions in inorganic ion concentrations, ALWC decreased dramatically in 2018/2019

227 (14.8 ± 20.4 μg m^{-3}), compared to that in 2015/2016 (24.4 ± 27.0 μg m^{-3}). In short, anthropogenic pollutant emissions, as well

228 as aerosol concentration and composition varied significantly between 2015/2016 and 2018/2019 in Shanghai, which, as will

229 be discussed below, has important implications for the production of OS in ambient aerosols.

3.2 Molecular composition of sulfur-containing organic compounds

231 The organic compounds in ambient $PM_{2.5}$ identified using UPLC-ESI(-)-QToF-MS were classified into four groups based on

232 their elemental composition, i.e., CHO, CHON, CHOS, and CHONS. Figure 3a, b show the average mass spectra of organic

233 compounds in $PM_{2.5}$ over a typical winter (21-26 January 2019) and summer (23-28 July 2019) pollution episode. The S-

234 containing compounds were overall larger in molecular size than CHO and CHON compounds, likely because of the addition

235 of a sulfate group to the molecule. The molecular weight (MW) of most S-containing compounds was between 100-400 Da,

236 and a few between 400-700 Da. The high-MW CHOS species (400-700 Da, see Table S4) showed a larger contribution in

237 winter than in summer, suggesting that they are more likely to arise from anthropogenic sources than biogenic emissions.

238 Figure 3c shows the signal contribution of different compound categories as well as concentrations of sulfate, OM, and

239 quantified OS, and Fig. 3d, e shows the number of identified organic compounds in each category during two pollution

240 episodes. The CHOS compounds contributed most by signal and number to observed organic compounds in both winter and

241 summer. The signal contributions and number of unquantified CHOS and CHONS did not vary significantly from winter to

242 summer, whereas the signal contribution of quantified CHOS and CHONS species were significantly larger in summer than

243 in winter (on average 15% vs. 7% for CHOS and 11% vs. 7% for CHONS). As will be discussed later, the abundance of

244 quantified anthropogenic OS was fairly constant across different seasons, in striking contrast to biogenic OS that showed

245 strong seasonal variability. Therefore, lack of seasonal variability for unquantified CHOS and CHONS implies that they may

246 originate mainly from anthropogenic sources. In addition, both signal intensity and the number of CHO species increased

247 significantly in summer, compared to those in winter. In contrast, CHON compounds contributed substantially more to the

248 observed signals in winter than in summer (on average 25% vs. 7%), though their numbers are quite similar during the two

249 periods. This suggests an enhanced production and/or suppressed depletion of nitrogen-containing organic species in winter.

The CHOS compounds with an O/S ratio of ≥ 4 were assigned as potential OS species. Similarly, the CHONS compounds with an O/(N+S) ratio of ≥ 7 could be assigned as potential NOS species (Lin et al., 2012a). The $C_8H_{17}O_4S^-$, $C_8H_{15}O_4S^-$, and $C_5H_{11}O_4S^-$ were the highest OS peaks observed in the pollution episode in winter. The $C_8H_{17}O_4S^-$ and $C_8H_{15}O_4S^-$ species may be derived from the photooxidation of diesel fuel vapors according to previous chamber studies (Blair et al., 2017). The $C_5H_{11}O_4S^-$ species was correlated well with $C_8H_{17}O_4S^-$ in 2015/2016 (r=0.76) and 2018/2019 (r=0.84), suggesting it may also be derived from diesel fuel vapors. The highest NOS peak in winter is $C_{10}H_{16}NO_7S^-$, which likely originate from monoterpene oxidation (Surratt et al., 2008). The $C_5H_{11}O_7S^-$, $C_{15}H_{29}O_5S^-$, and $C_{13}H_{25}O_5S^-$ were observed among the highest OS peaks in the summer pollution episode. The $C_5H_{11}O_7S^-$ is an IEPOX-derived OS species (Surratt et al., 2010), while $C_{15}H_{29}O_5S^-$ and $C_{13}H_{25}O_5S^-$ may be derived from the oxidation of diesel fuel vapors (Blair et al., 2017). The highest NOS peak in summer is monoterpene-derived $C_{10}H_{16}NO_7S^-$, the same with that in winter.

3.3 Quantified organosulfates

In this study, we quantified twenty-nine OS and six NOS compounds using a variety of authentic and surrogate OS standards (Table 1). The quantified OS and NOS accounted for 14-18% and 47-67% by intensity of identified CHOS and CHONS in polluted winter days and 15-37% and 58-87%, in polluted summer days (Fig. 3c), respectively. Increased contribution of the quantified OS and NOS in summer is because they are mainly derived from biogenic VOCs, which have greater emissions in summer than in other seasons (Guenther et al., 1995). We note that a large fraction of OS signals were not quantified owing to the lack of proper standards in this study. As discussed above, these unquantified OS mainly originated from anthropogenic sources. Future studies of their abundances and formation mechanisms are warranted.

Table 2 summarizes the seasonally and annually averaged concentrations of the quantified OS, as well as their contributions to OM in 2015/2016 and 2018/2019. The average concentration of quantified OS was 65.5±77.5 ng m^{-3} in 2015/2016 and 59.4±79.7 ng m^{-3} in 2018/2019. Although there was little change in OS concentration in these two years, the contribution of OS to OM was larger in 2018/2019 (0.66%±0.56%) than in 2015/2016 (0.57%±0.56%), mainly due to a significant reduction of OM in 2018/2019. Since OS species are important tracers for SOA (Surratt et al., 2007b; Gomez-Gonzalez et al., 2008; Surratt et al., 2008; McNeill et al., 2012; Zhang et al., 2012; Surratt et al., 2010; Lin et al., 2013), an increase of OS/OM ratios in 2018/2019 implies an enhanced contribution of SOA to OA in Shanghai. A previous study by Ma et al. (2014) reported an average OS concentration in urban Shanghai in 2012/2013 of about 8.6 ng m^{-3}, substantially smaller than the concentration reported here. This is likely due to a different number of OS species quantified (17 vs. 35) and different OS standards used (octyl and benzyl sulfates vs. seven authentic/surrogate standards) in Ma et al. (2014) and the present study. As can be seen in Fig. 2e and Table 2, the OS concentration and OS/OM ratio both showed a strong seasonal variation and peaked in summer. The concentration of OS and its contribution to OM in summertime Shanghai (on average, 114.1 ng m^{-3} and 1.13% in July 2015 and 102.1 ng m^{-3} and 1.18% in July 2019) were larger or comparable to those observed in Beijing (55.2 ng m^{-3}, 0.42%) (Wang et al., 2018) and Birmingham, Alabama (205.4 ng m^{-3}, 2% of OC) (Rattanavaraha et al., 2017), but significantly lower than those observed in Atlanta, GA (2366.4 ng m^{-3}, 16.5% of OC) and Centreville, AL (812 ng m^{-3}, 7.3% of OC) (Hettiyadura et al., 2019) where the production of OS and SOA is dominated by the oxidation of biogenic emissions. The contribution of OS to OM in wintertime Shanghai (on average, 0.32% in January 2016 and 0.36% in January 2019) was larger than that

observed in Xi'an (~0.2%) (Huang et al., 2018), though the quantified OS concentrations in two regions were comparable. This may suggest a stronger secondary formation of OA in Shanghai than in Xi'an, consistent with independent measurements by Huang et al. (2014).

To further characterize the seasonality and interannual variability of OS, as well as their origin and formation mechanisms, the quantified OS were assigned to four different source categories based on their molecular composition and literature data (Surratt et al., 2008; Surratt et al., 2007a; Nozière et al., 2010; Surratt et al., 2010; Schindelka et al., 2013; Zhang et al., 2014; Riva et al., 2015; Riva et al., 2016b; Blair et al., 2017; Nestorowicz et al., 2018). The OS species for each OS source category are listed in Table 1 and the seasonal and interannual variations in the abundance of grouped and individual OS are shown in Fig. 4 and Table S5, respectively.

3.3.1 Isoprene-derived organosulfates

Isoprene-derived OS (hereafter referred to as OS_i) include ten C_{4-5} species and one dimeric species ($C_7H_9O_7S^-$). The average concentration of OS_i in summer was 76.5 ± 93.4 ng m^{-3} for 2015/2016 and 68.4 ± 102.2 ng m^{-3} for 2018/2019, significantly larger than the concentrations (10.4-17.1 ng m^{-3}) in other seasons (Fig. 4a). Similar strong seasonality of OS_i was also observed in suburban areas in the Mid-Atlantic United States (Meade et al., 2016) and the Pearl River Delta in Southern China (He et al., 2014) The significantly increased production of OS_i in summer is mainly a result of enhanced isoprene emissions (Guenther et al., 1995) and photochemistry due to strong solar radiation and high temperatures in this warmer season.

The most abundant species among OS_i was 2-MT-OS ($C_5H_{11}O_7S^-$), produced by reactive uptake of IEPOX on sulfate during the photooxidation of isoprene under low-NO_x conditions (Surratt et al., 2010). The average concentration of 2-MT-OS was ~31 ng m^{-3} in summer, contributing to about 45% of OS_i, whereas it decreased to 0.4-1.3 ng m^{-3} in other seasons, accounting for only 4-10% of OS_i in 2015/2016 and 2018/2019 (see Table S5). In addition, 2-MA-OS ($C_4H_7O_7S^-$) was also abundantly detected with an average concentration of 4.5 ng m^{-3} in summer and 1.0-2.2 ng m^{-3} in other seasons during the two sampling years. 2-MA-OS is formed from reactive uptake of methacrylic acid epoxide (MAE) (Lin et al., 2013) and hydroxymethyl-methyl-lactone (HMML) (Nguyen et al., 2015) on sulfate aerosol during isoprene photooxidation under high-NO_x conditions. It is worthwhile noting that the concentration ratio of 2-MT-OS/2-MA-OS in summer (6.8-7.8) is substantially larger than that in other seasons (0.31-0.78). This is consistent with a dramatic reduction of NO_x level (e.g., NO_2) in summer (~13 ppb) compared to that in other seasons (~24-34 ppb) (see Table S1). Furthermore, the NO_x-influenced oxidation pathways may not be conducive to 2-MA-OS formation in summer, given that the formation of reactive intermediates such as MAE is unfavorable at high temperatures owing to enhanced thermal decomposition of its precursor methacryloylperoxynitrate (MPAN) (Worton et al., 2013). Since 2-MT-OS and 2-MA-OS are key tracers for isoprene-derived SOA under low- and high-NO_x conditions, respectively (Surratt et al., 2010; Lin et al., 2013; Nguyen et al., 2015). The dramatically larger ratios of 2-MT-OS/2-MA-OS in summer than in other seasons therefore strongly suggests that the low-NO_x oxidation pathways dominated the production of isoprene-derived SOA in summer, while the processes favorable under high-NO_x conditions were important SOA formation in other seasons. We note that the 2-MT-OS/2-MA-OS ratios observed in summertime Shanghai are smaller than those (17.0-33.8) observed in less polluted environments such as the southeastern United States (Hettiyadura et al., 2019; Budisulistiorini et al., 2015; Riva et al., 2019), but significantly larger than those (0.55-1.57) observed in Beijing

320 (Wang et al., 2018; Bryant et al., 2020) and the Pearl River Delta (PRD) region of China (He et al., 2018).

321 Other abundant OS_i species include $C_5H_7O_7S^-$, $C_5H_9O_7S^-$, and $C_4H_7O_6S^-$. The $C_5H_7O_7S^-$ and $C_5H_9O_7S^-$ species can be produced

322 by photooxidation of isoprene (Surratt et al., 2008; Nestorowicz et al., 2018) and/or the oxidative aging of 2-MT-OS

323 (Hettiyadura et al., 2015; Chen et al., 2020). The $C_4H_7O_6S^-$ can be generated both from sulfate radical reaction with

324 MACR/MVK (Nozière et al., 2010; Schindelka et al., 2013; Wach et al., 2019) and isoprene photooxidation (Lin et al., 2013;

325 Surratt et al., 2007a; Nestorowicz et al., 2018). The $C_5H_7O_7S^-$ and $C_4H_7O_6S^-$ are also consistent in molecular formula with the

326 OS species formed from the photooxidation of diesel fuel vapors (Blair et al., 2017). However, these two species had moderate

327 to strong correlations with MT-OS and $C_5H_9O_7S^-$ in different seasons expect for autumn ($C_5H_7O_7S^-$: r=0.68-0.96, $C_4H_7O_6S^-$:

328 r=0.62-0.96), indicating that they are mainly derived from isoprene oxidation. We note that the five most abundant OS_i species

329 as discussed above were moderately correlated with EC and CO in winter (r=0.5-0.67), suggesting that there might be

330 anthropogenic sources of isoprene in winter. Borbon et al. (2001) measured the hourly isoprene concentration at an urban site

331 in Lille, France for two years and found that isoprene was largely derived from vehicle emissions in winter. In addition to OS

332 species, two isoprene-derived NOSs ($C_5H_{10}NO_9S^-$ and $C_5H_8NO_{10}S^-$) were also observed, in particular in summer.

333 **3.3.2 Monoterpene-derived organosulfates**

334 Monoterpene-derived OS (hereafter referred to as OS_m) include seven C_{7-10} OS species and three C_{9-10} NOS species. Compared

335 to the OS_i, the OS_m showed a weaker seasonal variation and a relatively larger abundance except in summer (Fig. 4b). This is

336 consistent with the fact that isoprene emissions have stronger seasonal variability than monoterpene emissions (Guenther et

337 al., 1995). The seasonally averaged concentrations of OS_m were higher in spring and summer, but lower in autumn and winter.

338 This is different from previous observations in 2012/2013 in Shanghai by Ma et al (2014). They found that the OS_m were

339 most abundant in summer, followed by autumn, winter, and spring. The differences in seasonal variations of OS_m observed

340 by the two studies may be attributed to different meteorological and chemical conditions that affected precursor emissions

341 and chemistry of OS_m formation over the sampling periods. Given that the OS_m concentration had an obvious daily variation,

342 the number of samples collected would significantly affect the seasonally averaged concentration. As such, the difference in

343 the number of samples collected each season (18-20 samples in this study versus 6 samples within three days in Ma et al.

344 (2014)) may also contribute to the different seasonality observed in two studies.

345 The NOS species such as $C_{10}H_{16}NO_7S^-$, $C_9H_{14}NO_8S^-$, and $C_{10}H_{16}NO_{10}S^-$ were the most abundant OS_m species, which arises

346 mainly from monoterpenes photooxidation in the presence of NO_x or nighttime NO_3 chemistry (Surratt et al., 2008; Iinuma

347 et al., 2007a). The concentrations of these three NOS were all lower in summer than in spring and autumn (Table S5),

348 consistent with the seasonal trend of NO_x concentrations (Fig. 2 and Table S1). Similar seasonal variations for these NOS

349 species were also observed in the PRD region of China (He et al., 2014) and the Mid-Atlantic United States (Meade et al.,

350 2016). Among NOS species, the $C_{10}H_{16}NO_7S^-$ was most abundant, contributing to 22-48% of OS_m. This species had an annual

351 average concentration of 6.2±6.5 ng m^{-3} in 2015/2016 and 5.5±6.2 ng m^{-3} in 2018/2019, which is comparable to the

352 concentrations observed in Beijing (12 ng m^{-3}) (Wang et al., 2018) and Atlanta, GA (9.0 ng m^{-3}) (Hettiyadura et al., 2019),

353 but much lower than observed in the PRD region of China (52.4 ng m^{-3} in summer and 151 ng m^{-3} in autumn) (He et al.,

354 2014). The prevalence of monoterpene-derived NOS in Shanghai as observed in this study is consistent with recent

observations that monoterpenes accounted for up to 60% of nighttime NO_3 radical loss in the YRD region of China (Wang et al., 2020a).

The most abundant nitrogen-free OS_m species was $C_{10}H_{15}O_7S^-$ (m/z 279.0538), which was shown to be produced from the photooxidation of monoterpenes (Surratt et al., 2008) or sulfate radical reaction with α-pinene (Nozière et al., 2010). Although the $C_{10}H_{15}O_7S^-$ is consistent in molecular composition with the OS species formed by photooxidation of cyclodecane in the presence of sulfate aerosol (Riva et al., 2016b), its moderate to strong correlation (r=0.51-0.93) with the three monoterpene-derived NOS in all seasons except for winter suggests that it is mainly derived from monoterpene oxidation. The concentration of $C_{10}H_{15}O_7S^-$ was on average 3.0 ± 3.0 ng m^{-3} in 2015/2016, lower than that (4.0 ± 3.4 ng m^{-3}) in 2018/2019. In contrast to NOS species, the $C_{10}H_{15}O_7S^-$ species was most abundant in summer in both years, again suggesting a strong contribution of low-NO_x chemistry in OS and SOA formation in summer.

3.3.3 Anthropogenic organosulfates

The quantified anthropogenic OS (hereafter referred to as OS_a) in this study include phenyl sulfate ($C_6H_5O_4S^-$), benzyl sulfate ($C_7H_7O_4S^-$), $C_8H_{17}O_4S^-$, as well as $C_4H_7O_4S^-$, $C_5H_7O_6S^-$, and $C_6H_9O_6S^-$. The annual average concentrations of OS_a in 2015/2016 and 2018/2019 were 5.6±2.8 ng m^{-3} and 3.8±3.3 ng m^{-3}, respectively. Although the concentration of quantified OS_a decreased in 2018/2019, we are not sure whether the total concentration of OS_a decreased because only a small fraction of OS_a were quantified. The inter-annual variations of OS_a warrants further studies. As shown in Fig. 4c, the quantified OS_a concentration was substantially smaller compared to biogenic OS. In addition, the OS_a concentration had little seasonal variations in both 2015/2016 and 2018/2019. Among quantified OS_a, the $C_4H_7O_4S^-$ was most abundant with an annual average concentration of 2.0±1.5 ng m^{-3} in 2015/2016 and 1.8±2.6 ng m^{-3} in 2018/2019, which is comparable to the concentrations in Atlanta,GA (Hettiyadura et al., 2019). Blair et al. (2017) found that photooxidation of diesel vapors in the presence of SO_2 can form $C_4H_7O_4S^-$, $C_5H_7O_6S^-$, and $C_6H_9O_6S^-$ species. The $C_8H_{17}O_4S^-$ species had the same retention time with the octyl sulfate standard in the LC column, suggesting it is a long-chain aliphatic OS. This OS species was correlated with $C_5H_7O_6S^-$ and $C_6H_9O_6S^-$ that were potential diesel vapor-derived OS. Phenyl sulfate and benzyl sulfate may be produced by photooxidation of naphthalene and 2-methylnaphthalene (Riva et al., 2015) and/or sulfate radical reaction with aromatic compounds such as benzoic acid and toluene in the aqueous phase (Huang et al., 2020), but phenyl sulfate was only detected in 42 out of 75 samples in 2015/2016 and 8 out of 81 samples in 2018/2019, primarily in winter. The benzyl sulfate concentrations in 2015/2016 and 2018/2019 were 0.4±0.1 ng m^{-3} and 0.2±0.10 ng m^{-3}, respectively, which were higher than the observations in springtime Lahore, Pakistan (Staudt et al., 2014) and in wintertime Xi'an, China (Huang et al., 2018). Benzyl sulfate had a strong correlation with phenyl sulfate and was also correlated with $C_6H_9O_6S^-$ and $C_8H_{17}O_4S^-$.

3.3.4 C_2/C_3 organosulfates

The OS species with two or three carbon atoms are grouped together since many of them are considered to have both biogenic and anthropogenic origins. The C_2/C_3 OS quantified in this study include $C_2H_3O_6S^-$ (m/z 154.9650), $C_3H_5O_5S^-$ (m/z 152.9858), $C_3H_5O_6S^-$ (m/z 168.9807), $C_2H_3O_5S^-$ (m/z 138.9701), $C_3H_5O_4S^-$ (m/z 136.9909), and $C_3H_7O_5S^-$ (m/z 155.0014). The C_2/C_3 OS species averagely accounted for 19% of quantified OS concentrations and they were overall more abundant in summer

389 than in other seasons in 2015/2016 and 2018/2019 (Fig. 4d). The $C_2H_3O_6S^-$, $C_3H_5O_5S^-$, and $C_3H_5O_6S^-$ species, which were

390 previously assigned to glycolic acid sulfate (GAS), hydroxyacetone sulfate (HAS), and lactic acid sulfate (LAS), respectively

391 (Olson et al., 2011; Hettiyadura et al., 2017; Huang et al., 2018; Wang et al., 2018; Hettiyadura et al., 2019), were among the

392 most abundant C_2/C_3 OS species, together contributing to 76% of C_2/C_3 OS concentrations during the two sampling years.

393 The concentration of $C_2H_3O_6S^-$ (GAS) was on average 2.9±2.2 ng m^{-3} in 2015/2016 and 2.3±1.7 ng m^{-3} in 2018/2019, which

394 was lower than the concentrations measured in Beijing (19.5 ng m^{-3}) (Wang et al., 2018), Xi'an (77.3 ng m^{-3}) (Huang et al.,

395 2018), Atlanta, GA (58.5 ng m^{-3}) (Hettiyadura et al., 2019), Centreville, AL (20.6 ng m^{-3}) (Hettiyadura et al., 2017), Lahore,

396 Pakistan (11.3 ng m^{-3}), and Bakersfield, CA (4.5-5.4 ng m^{-3}) (Olson et al., 2011), and similar with those observed in Riverside,

397 CA (3.3 ng m^{-3}) (Olson et al., 2011). We note that if accounting for the underestimation (2-6 times) in concentration due to

398 matrix effects (see Sect. 2.5), the GAS concentration measured in Shanghai would be comparable to that in most of the regions

399 mentioned above. The concentrations of $C_3H_5O_5S^-$ (HAS) and $C_3H_5O_6S^-$ (LAS) were quite similar, on average 2.3 and 2.2 ng

400 m^{-3} in 2015/2016 and 1.8 and 1.9 ng m^{-3} in 2018/2019, respectively, which were comparable to the concentrations observed

401 in Beijing (2.2 ng m^{-3} and 4.4 ng m^{-3}) (Wang et al., 2018), and Xi'an (1.3 ng m^{-3} for HAS) (Huang et al., 2018), but lower than

402 those measured in Centreville, AL (5.8 ng m^{-3} and 16.5 ng m^{-3}) (Hettiyadura et al., 2017) and Atlanta, GA (10.1 ng m^{-3} and

403 38.4 ng m^{-3}) (Hettiyadura et al., 2019). The $C_2H_3O_6S^-$, $C_3H_5O_5S^-$, $C_3H_5O_6S^-$, and $C_2H_3O_5S^-$ were strongly correlated with most

404 of OS$_i$ species (r=0.52-0.96 for $C_2H_3O_6S^-$, r=0.53-0.99 for $C_3H_5O_5S^-$, r=0.53-0.90 for $C_3H_5O_6S^-$, and r=0.53-0.94 for

405 $C_2H_3O_5S^-$), indicating that they originated mainly from isoprene chemistry. This is in line with recent findings that a series of

406 C_2/C_3 OS species, including $C_2H_3O_6S^-$, $C_3H_5O_6S^-$, and $C_2H_3O_5S^-$, can be produced by heterogeneous OH oxidation of

407 particulate 2-MT-OS (Chen et al., 2020). The $C_3H_5O_4S^-$ species, proposed to contain an allyl group (Hettiyadura et al., 2017),

408 was previously found to be produced by diesel photooxidation (Blair et al., 2017), and was correlated with anthropogenic OS

409 such as the potential diesel vapor-derived OS ($C_8H_{17}O_4S^-$, $C_4H_7O_4S^-$, $C_5H_7O_6S^-$, and $C_6H_9O_6S^-$, r=0.53-0.87) and benzyl

410 sulfate ($C_7H_7O_4S^-$, r=0.49-0.88). The $C_3H_7O_5S^-$ is likely an OS species containing one hydroxyl group (Hettiyadura et al.,

411 2017), which was strongly correlated with the $C_3H_5O_4S^-$ in all seasons and correlated with the diesel vapor-derived OS$_a$

412 ($C_6H_9O_6S^-$ and $C_8H_{17}O_4S^-$) in spring and autumn, suggesting that it may be largely derived from the photooxidation of diesel

413 vapors. This result is different from the observations in Atlanta, GA, where the $C_3H_7O_5S^-$ was correlated with most of OS$_i$,

414 leading to the suggestion that it was derived from the oxidation of isoprene (Hettiyadura et al., 2019). We note that the

415 concentrations of $C_3H_5O_4S^-$ and $C_3H_7O_5S^-$ species decreased significantly from 2015/2016 to 2018/2019 (except for summer,

416 see Table S5), overall consistent with the interannual variations of OS$_a$ species. This further supports that these two OS species

417 mainly originated from anthropogenic sources.

418 **3.4 Factors influencing organosulfate formation**

419 Laboratory and field studies have shown that aerosol properties such as acidity, sulfate concentration, and ALWC play

420 important roles in the formation of OS (Iinuma et al., 2007b; Chan et al., 2011; Surratt et al., 2007a; Surratt et al., 2007b; Liao

421 et al., 2015; Hettiyadura et al., 2019; Riva et al., 2019). Here we examined the influences of these factors, as well as the level

422 of oxidants and temperature on OS formation in ambient aerosols in Shanghai. Aerosol pH and ALWC here were calculated

423 using ISORROPIA-II (see Sect. 2.4). Figure 5 shows the OS concentration versus the O$_x$ level, sulfate concentration, aerosol

424 pH, and ALWC observed in the spring, autumn, and winter of 2015-2016 and 2018-2019. Since the OS concentrations in

summer were significantly greater than in other seasons, they were plotted separately in Fig. 6. As shown in Figs. 5 and 6, the aerosol pH in Shanghai ranged between 1.5 and 5.3 in summer and between 2.5 and 6.1 in other seasons, overall within the pH range (2-6) reported for ambient aerosols in northern China (Liu et al., 2017; Shi et al., 2017; Ding et al., 2019b; Song et al., 2019; Wang et al., 2018). A recent study by Zheng et al. (2020) has suggested that aerosol pH levels in populated continental regions including eastern and northern China are widely buffered by ammonium/ammonia, where the variation in aerosol pH is mainly driven by the variation in ALWC and temperature. Therefore, we infer that the lower aerosol pH in summer than in other seasons in Shanghai was mainly a result of decreased ALWC (Figs. 5 and 6c, d) and enhanced temperature (Fig. 2a). Decreased aerosol pH in summer compared to other seasons were also observed in Beijing (Ding et al., 2019b) and the southeastern United States (Guo et al., 2015; Nah et al., 2018).

As can be seen in Fig. 5, the OS concentration in spring, autumn, and winter increased obviously with increasing O_x level, sulfate concentration, and aerosol acidity (Fig. 5a, b). A similar result was also found in Beijing that most OS species were correlated strongly with the product of ozone and particulate sulfate ($[O_3] \cdot [SO_4^{2-}]$) (Bryant et al., 2020). In addition, an overall positive correlation was observed between the OS concentration and ALWC (Fig. 5c, d). Therefore, it is likely that that the OS species were mainly produced by acid-catalyzed heterogeneous/aqueous-phase reactions of oxidized organic compounds with sulfate in these seasons. Previous studies have shown that elevated ALWC could inhibit OS production by decreasing aerosol acidity through dilution (Lewandowski et al., 2015; Nestorowicz et al., 2018). However, as the increase of ALWC was accompanied by elevated sulfate concentration, such a decrease in aerosol acidity was not observed in the present study (Fig. 5c, d). Alternatively, the increased ALWC likely promoted the mass transfer of oxidized organics into the aerosol phase, thereby enhancing OS formation. We note that the observations with moderate to high ALWC but relatively low OS concentration (data points in the triangle in Fig. 5c, d) were associated with low O_x levels (<50 ppb) that significantly limited the oxidation of VOC precursors and hence the formation of OS.

As seen in Fig. 6, OS production in summer increased dramatically with rising O_x concentration. In addition, high OS concentrations were associated with high ambient temperatures, which can enhance emissions of biogenic precursors and the production of O_x. While the aerosol acidity effect on OS production in summer was still evident, the influence of sulfate and ALWC was not as obvious as in other seasons. This is likely because the OS production in summer was driven by the strong emission and fast photochemistry of VOC precursors. It is noteworthy that the sulfate concentrations, ALWC, and aerosol acidities were overall higher in 2015/2016 than in 2018/2019, but the OS concentrations were similar in two years. This implies that the O_x level is a driving factor for OS formation in ambient aerosols in Shanghai. Very recently, a similar oxidant effect on OS formation was also observed in urban Beijing (Bryant et al., 2020). Therefore, mitigation of O_x pollution may effectively reduce the production of OS and SOA in Chinese megacities.

4 Conclusions

In this study, we collected ambient $PM_{2.5}$ filter samples over four seasons in 2015/2016 and 2018/2019 in urban Shanghai, China, and comprehensively characterized the sulfur-containing organic compounds (CHOS and CHONS) in these $PM_{2.5}$ samples using UPLC-ESI(-)-QToF-MS. The CHOS and CHONS species accounted for a large fraction of ion signals for organic compounds in ambient $PM_{2.5}$. Using a set of authentic and surrogate OS standards, we quantified the abundance of

460   29 OS and 6 NOS species in ambient aerosols. We find that there was no strong change in the OS concentration in 2018/2019

461   (59.4 ± 79.7 ng m^{-3}) compared to that in 2015/2016 (65.5 ± 77.5 ng m^{-3}), though the OM concentration decreased by 29%

462   between 2015/2016 (12.7 ± 8 μg m^{-3}) and 2018/2019 (9 ± 5.5 μg m^{-3}). As a result, the annual average contribution of quantified

463   OS to OM increased from 0.57% in 2015/2016 to 0.66% in 2018/2019, suggesting an enhanced contribution of SOA to OM

464   in Shanghai in recent years. The OS$_i$ and OS$_m$ on average accounted for 36.3% and 31.0% of the quantified OS concentrations,

465   respectively, during the two sampling years, indicating a significant contribution of biogenic emissions to SOA in Shanghai.

466   The abundance of OS$_i$ had strong seasonality and was significantly higher in summer (76.5 ± 93.4 ng m^{-3} in 2015/2016 and

467   68.4 ± 102.2 ng m^{-3} in 2018/2019) than in other seasons (10.4-17.1 ng m^{-3}). The OS$_m$ concentration showed a weaker seasonal

468   variation and was relatively higher in spring and summer than in autumn and winter. In contrast, the quantified OS$_a$ had little

469   seasonal variations and decreased by 32% from 2015/2016 to 2018/2019. The C$_2$/C$_3$ OS species that were more abundant in

470   summer than in other seasons, on average contributed to 19% of the concentration of quantified OS species. The C$_2$H$_3$O$_6$S$^-$

471   (GAS), C$_3$H$_5$O$_5$S$^-$ (HAS), and C$_3$H$_5$O$_6$S$^-$ (LAS), which were derived mainly from isoprene chemistry, were the most abundant

472   C$_2$/C$_3$ OS species and together accounted for 76% of C$_2$/C$_3$ OS concentrations.

473   2-MT-OS was the most abundant OS species in summer. The dramatic larger 2-MT-OS/2-MA-OS ratios in summer (6.8-7.8)

474   versus other seasons (0.31-0.78) implies that the reaction pathways prevalent under low-NO$_x$ conditions (e.g., reactive uptake

475   of IEPOX and photooxidation of ISOPOOH) dominated the production of OS$_i$ and isoprene-derived SOA in summer, while

476   the processes favorable under high-NO$_x$ conditions play an important role in OS$_i$ and SOA formation in other seasons. The

477   C$_{10}$H$_{16}$NO$_7$S$^-$ species derived from monoterpenes was the most abundant NOS species, with an annual average concentration

478   of 6.2 ± 6.5 ng m^{-3} in 2015/2016 and 5.5 ± 6.2 ng m^{-3} in 2018/2019. This agrees well with previous observations that

479   monoterpenes depleted about 60% of nighttime NO$_3$ radicals in the YRD region of China (Wang et al., 2020a).

480   In addition, we find that the abundance of OS was overall positively correlated with the O$_x$ level, sulfate concentration, aerosol

481   acidity, as well as ALWC in spring, autumn, and winter, suggesting the production of OS via acid-catalyzed aqueous-phase

482   reactions of oxidized organic compounds on sulfate. However, OS production in summer was strongly driven by rising O$_x$

483   and temperature that could enhance the photochemistry and emissions of biogenic precursors. We further find that although

484   sulfate concentrations, aerosol acidities, and ALWC were significantly lower in 2018/2019 than in 2015/2016, the production

485   of OS was largely sustained in 2018/2019 by the nearly unchanged O$_x$ level that maintained the fast oxidation of VOC

486   precursors. These results imply that controlling O$_x$ pollution may also effectively mitigate particulate organic matter pollution

487   in eastern China.

488   It should be pointed out that GAS was likely underestimated by a factor of 2-6 as a result of the matrix effect during the

489   analysis in our study. If accounting for this effect, it would be the second most abundant OS species after MT-OS. In addition,

490   a large fraction of CHOS signals that arose mainly from anthropogenic sources were not quantified due to the lack of proper

491   OS standards in this study. Therefore, the OS concentration and its contribution to organic aerosol in Shanghai could be

492   significantly greater. Future studies on the abundance, origin, and formation mechanisms of these unquantified OS are

493   warranted for a better understanding of the formation and evolution of OS and SOA in the atmosphere.

494

References

Behera, S. N., Cheng, J., Huang, X., Zhu, Q., Liu, P., and Balasubramanian, R.: Chemical composition and acidity of size-fractionated inorganic aerosols of 2013-14 winter haze in Shanghai and associated health risk of toxic elements, Atmos. Environ., 122, 259-271, 10.1016/j.atmosenv.2015.09.053, 2015.

Blair, S. L., MacMillan, A. C., Drozd, G. T., Goldstein, A. H., Chu, R. K., Pasa-Tolic, L., Shaw, J. B., Tolic, N., Lin, P., Laskin, J., Laskin, A., and Nizkorodov, S. A.: Molecular Characterization of Organosulfur Compounds in Biodiesel and Diesel Fuel Secondary Organic Aerosol, Environ. Sci. Technol., 51, 119-127, 10.1021/acs.est.6b03304, 2017.

Borbon, A., Fontaine, H., Veillerot, M., Locoge, N., Galloo, J. C., and Guillermo, R.: An investigation into the traffic-related fraction of isoprene at an urban location, Atmos. Environ., 35, 3749-3760, 2001.

Brüggemann, M., Poulain, L., Held, A., Stelzer, T., Zuth, C., Richters, S., Mutzel, A., van Pinxteren, D., Iinuma, Y., Katkevica, S., Rabe, R., Herrmann, H., and Hoffmann, T.: Real-time detection of highly oxidized organosulfates and BSOA marker compounds during the F-BEACh 2014 field study, Atmos. Chem. Phys., 17, 1453-1469, 10.5194/acp-17-1453-2017, 2017.

Brüggemann, M., Xu, R. S., Tilgner, A., Kwong, K. C., Mutzel, A., Poon, H. Y., Otto, T., Schaefer, T., Poulain, L., Chan, M. N., and Herrmann, H.: Organosulfates in ambient aerosol: state of knowledge and future research directions on formation, abundance, fate, and importance, Environ. Sci. Technol., 54, 3767-3782, doi: 10.1021/acs.est.9b06751, 2020.

Bryant, D. J., Dixon, W. J., Hopkins, J. R., Dunmore, R. E., Pereira, K. L., Shaw, M., Squires, F. A., Bannan, T. J., Mehra, A., Worrall, S. D., Bacak, A., Coe, H., Percival, C. J., Whalley, L. K., Heard, D. E., Slater, E. J., Ouyang, B., Cui, T., Surratt, J. D., Liu, D., Shi, Z., Harrison, R., Sun, Y., Xu, W., Lewis, A. C., Lee, J. D., Rickard, A. R., and Hamilton, J. F.: Strong anthropogenic control of secondary organic aerosol formation from isoprene in Beijing, Atmos. Chem. Phys., 20, 7531-7552, 10.5194/acp-20-7531-2020, 2020.

Budisulistiorini, S. H., Li, X., Bairai, S. T., Renfro, J., Liu, Y., Liu, Y. J., McKinney, K. A., Martin, S. T., McNeill, V. F., Pye, H. O. T., Nenes, A., Neff, M. E., Stone, E. A., Mueller, S., Knote, C., Shaw, S. L., Zhang, Z., Gold, A., and Surratt, J. D.: Examining the effects of anthropogenic emissions on isoprene-derived secondary organic aerosol formation during the 2013 Southern Oxidant and Aerosol Study (SOAS) at the Look Rock, Tennessee ground site, Atmos. Chem. Phys., 15, 8871-8888, 10.5194/acp-15-8871-2015, 2015.

Chan, M. N., Surratt, J. D., Claeys, M., Edgerton, E. S., Tanner, R. L., Shaw, S. L., Zheng, M., Knipping, E. M., Eddingsaas, N. C., Wennberg, P. O., and Seinfeld, J. H.: Characterization and quantification of isoprene-derived epoxydiols in ambient aerosol in the southeastern United States, Environ. Sci. Technol., 44, 4590-4596, 10.1021/es100596b, 2010.

Chan, M. N., Surratt, J. D., Chan, A. W. H., Schilling, K., Offenberg, J. H., Lewandowski, M., Edney, E. O., Kleindienst, T. E., Jaoui, M., Edgerton, E. S., Tanner, R. L., Shaw, S. L., Zheng, M., Knipping, E. M., and Seinfeld, J. H.: Influence of aerosol acidity on the chemical composition of secondary organic aerosol from beta-caryophyllene, Atmos. Chem. Phys., 11, 1735-1751, 10.5194/acp-11-1735-2011, 2011.

Chen, Y., Zhang, Y., Lambe, A. T., Xu, R., Lei, Z., Olson, N. E., Zhang, Z., Szalkowski, T., Cui, T., Vizuete, W., Gold, A., Turpin, B. J., Ault, A. P., Chan, M. N., and Surratt, J. D.: Heterogeneous hydroxyl radical oxidation of isoprene-epoxydiol-derived methyltetrol sulfates: plausible formation mechanisms of previously unexplained organosulfates in ambient fine aerosols, Environ. Sci. Technol. Lett., 7, 460-468, 10.1021/acs.estlett.0c00276, 2020.

Claeys, M., Wang, W., Vermeylen, R., Kourtchev, I., Chi, X., Farhat, Y., Surratt, J. D., Gomez-Gonzalez, Y., Sciare, J., and Maenhaut, W.: Chemical characterisation of marine aerosol at Amsterdam Island during the austral summer of 2006-2007, J. Aerosol Sci., 41, 13-22, 10.1016/j.jaerosci.2009.08.003, 2010.

Darer, A. I., Cole-Filipiak, N. C., O'Connor, A. E., and Elrod, M. J.: Formation and stability of atmospherically relevant isoprene-derived organosulfates and organonitrates, Environ. Sci. Technol., 45, 1895-1902, 10.1021/es103797z, 2011.

DeRieux, W.-S., Li, Y., Lin, P., Laskin, J., Laskin, A., Bertram, A. K., Nizkorodov, S. A., and Shiraiwa, M.: Predicting the glass

transition temperature and viscosity of secondary organic material using molecular composition, Atmos. Chem. Phys., 18, 6331-6351, 10.5194/acp-18-6331-2018, 2018.

Ding, A., Huang, X., Nie, W., Chi, X., Xu, Z., Zheng, L., Xu, Z., Xie, Y., Qi, X., Shen, Y., Sun, P., Wang, J., Wang, L., Sun, J., Yang, X.-Q., Qin, W., Zhang, X., Cheng, W., Liu, W., Pan, L., and Fu, C.: Significant reduction of PM2.5 in eastern China due to regional-scale emission control: evidence from SORPES in 2011-2018, Atmos. Chem. Phys., 19, 11791-11801, 10.5194/acp-19-11791-2019, 2019a.

Ding, J., Zhao, P. S., Su, J., Dong, Q., Du, X., and Zhang, Y. F.: Aerosol pH and its driving factors in Beijing, Atmos. Chem. Phys., 19, 7939-7954, 10.5194/acp-19-7939-2019, 2019b.

Estillore, A. D., Hettiyadura, A. P. S., Qin, Z., Leckrone, E., Wombacher, B., Humphry, T., Stone, E. A., and Grassian, V. H.: Water uptake and hygroscopic growth of organosulfate aerosol, Environ. Sci. Technol., 50, 4259-4268, 10.1021/acs.est.5b05014, 2016.

Fisseha, R., Dommen, J., Gutzwiller, L., Weingartner, E., Gysel, M., Emmenegger, C., Kalberer, M., and Baltensperger, U.: Seasonal and diurnal characteristics of water soluble inorganic compounds in the gas and aerosol phase in the Zurich area, Atmos. Chem. Phys., 6, 1895-1904, 10.5194/acp-6-1895-2006, 2006.

Fleming, L. T., Ali, N. N., Blair, S. L., Roveretto, M., George, C., and Nizkorodov, S. A.: Formation of light-absorbing organosulfates during evaporation of secondary organic material extracts in the presence of sulfuric acid, ACS Earth Space Chem., 3, 947-957, 10.1021/acsearthspacechem.9b00036, 2019.

Fountoukis, C. and Nenes, A.: ISORROPIA II: a computationally efficient thermodynamic equilibrium model for K^+-Ca^{2+}-Mg^{2+}-NH_4^+-Na^+-SO_4^{2-}-NO_3^--Cl^--H_2O aerosols, Atmos. Chem. Phys., 7, 4639-4659, 10.5194/acp-7-4639-2007, 2007.

Froyd, K. D., Murphy, S. M., Murphy, D. M., de Gouw, J. A., Eddingsaas, N. C., and Wennberg, P. O.: Contribution of isoprene-derived organosulfates to free tropospheric aerosol mass, P. Natl. Acad. Sci. USA, 107, 21360-21365, 10.1073/pnas.1012561107, 2010.

Gómez-González, Y., Surratt, J. D., Cuyckens, F., Szmigielski, R., Vermeylen, R., Jaoui, M., Lewandowski, M., Offenberg, J. H., Kleindienst, T. E., Edney, E. O., Blockhuys, F., Van Alsenoy, C., Maenhaut, W., and Claeys, M.: Characterization of organosulfates from the photooxidation of isoprene and unsaturated fatty acids in ambient aerosol using liquid chromatography/(-) electrospray ionization mass spectrometry, J. Mass Spectrom., 43, 371-382, 10.1002/jms.1329, 2008.

Grgic, I., Dovzan, A., Bercic, G., and Hudnik, V.: The effect of atmospheric organic compounds on the Fe-catalyzed S(IV) autoxidation in aqueous solution, J. Atmos. Chem., 29, 315-337, 10.1023/a:1005918912994, 1998.

Griffith, S. M., Huang, X. H. H., Louie, P. K. K., and Yu, J. Z.: Characterizing the thermodynamic and chemical composition factors controlling PM2.5 nitrate: Insights gained from two years of online measurements in Hong Kong, Atmos. Environ., 122, 864-875, 10.1016/j.atmosenv.2015.02.009, 2015.

Guenther, A., Hewitt, C. N., Erickson, D., Fall, R., Geron, C., Graedel, T., Harley, P., Klinger, L., Lerdau, M., McKay, W. A., Pierce, T., Scholes, B., Steinbrecher, R., Tallamraju, R., Taylor, J., and Zimmerman, P.: A global model of natural volatile organic compound emissions, J. Geophys. Res., 100, 8873-8892, doi: 10.1029/94JD02950, 1995.

Guo, H., Xu, L., Bougiatioti, A., Cerully, K. M., Capps, S. L., Hite, J. R., Carlton, A. G., Lee, S. H., Bergin, M. H., Ng, N. L., Nenes, A., and Weber, R. J.: Fine-particle water and pH in the southeastern United States, Atmos. Chem. Phys., 15, 5211-5228, 10.5194/acp-15-5211-2015, 2015.

Guo, H., Sullivan, A. P., Campuzano-Jost, P., Schroder, J. C., Lopez-Hilfiker, F. D., Dibb, J. E., Jimenez, J. L., Thornton, J. A., Brown, S. S., Nenes, A., and Weber, R. J.: Fine particle pH and the partitioning of nitric acid during winter in the northeastern United States, J. Geophys. Res. Atmos., 121, 10355-10376, 10.1002/2016jd025311, 2016.

Hansen, A. M. K., Kristensen, K., Nguyen, Q. T., Zare, A., Cozzi, F., Nøjgaard, J. K., Skov, H., Brandt, J., Christensen, J. H., Ström, J., Tunved, P., Krejci, R., and Glasius, M.: Organosulfates and organic acids in Arctic aerosols: speciation, annual variation and concentration levels, Atmos. Chem. Phys., 14, 7807-7823, 10.5194/acp-14-7807-2014, 2014.

Hansen, A. M. K., Hong, J., Raatikainen, T., Kristensen, K., Ylisirnio, A., Virtanen, A., Petaja, T., Glasius, M., and Prisle, N. L.: Hygroscopic properties and cloud condensation nuclei activation of limonene-derived organosulfates and their mixtures with ammonium sulfate, Atmos. Chem. Phys., 15, 14071-14089, 10.5194/acp-15-14071-2015, 2015.

Hatch, L. E., Creamean, J. M., Ault, A. P., Surratt, J. D., Chan, M. N., Seinfeld, J. H., Edgerton, E. S., Su, Y., and Prather, K. A.: Measurements of isoprene-derived organosulfates in ambient aerosols by aerosol time-of-flight mass spectrometry-part 2: temporal variability and formation mechanisms, Environ. Sci. Technol., 45, 8648-8655, 10.1021/es2011836, 2011.

Hawkins, L. N., Russell, L. M., Covert, D. S., Quinn, P. K., and Bates, T. S.: Carboxylic acids, sulfates, and organosulfates in processed continental organic aerosol over the southeast Pacific Ocean during VOCALS-REx 2008, J. Geophys. Res., 115, 10.1029/2009jd013276, 2010.

He, Q. F., Ding, X., Wang, X. M., Yu, J. Z., Fu, X. X., Liu, T. Y., Zhang, Z., Xue, J., Chen, D. H., Zhong, L. J., and Donahue, N. M.: Organosulfates from pinene and isoprene over the Pearl River Delta, South China: seasonal variation and implication in formation mechanisms, Environ. Sci. Technol., 48, 9236-9245, 10.1021/es501299v, 2014.

He, Q. F., Ding, X., Fu, X. X., Zhang, Y. Q., Wang, J. Q., Liu, Y. X., Tang, M. J., Wang, X. M., and Rudich, Y.: Secondary organic aerosol formation from isoprene epoxides in the Pearl River Delta, South China: IEPOX- and HMML-derived tracers, J. Geophys. Res.-Atmos., 123, 6999-7012, 10.1029/2017jd028242, 2018.

Hennigan, C. J., Izumi, J., Sullivan, A. P., Weber, R. J., and Nenes, A.: A critical evaluation of proxy methods used to estimate the acidity of atmospheric particles, Atmos. Chem. Phys., 15, 2775-2790, 10.5194/acp-15-2775-2015, 2015.

Herrmann, H.: Kinetics of aqueous phase reactions relevant for atmospheric chemistry, Chem. Rev., 103, 4691-4716, 10.1021/cr020658q, 2003.

Hettiyadura, A. P. S., Stone, E. A., Kundu, S., Baker, Z., Geddes, E., Richards, K., and Humphry, T.: Determination of atmospheric

608   organosulfates using HILIC chromatography with MS detection, Atmos. Meas. Tech., 8, 2347-2358, 10.5194/amt-8-2347-2015,
609   2015.
610 Hettiyadura, A. P. S., Jayarathne, T., Baumann, K., Goldstein, A. H., de Gouw, J. A., Koss, A., Keutsch, F. N., Skog, K., and Stone,
611   E. A.: Qualitative and quantitative analysis of atmospheric organosulfates in Centreville, Alabama, Atmos. Chem. Phys., 17,
612   1343-1359, 10.5194/acp-17-1343-2017, 2017.
613 Hettiyadura, A. P. S., Al-Naiema, I. M., Hughes, D. D., Fang, T., and Stone, E. A.: Organosulfates in Atlanta, Georgia: anthropogenic
614   influences on biogenic secondary organic aerosol formation, Atmos. Chem. Phys., 19, 3191-3206, 10.5194/acp-19-3191-2019,
615   2019.
616 Hoffmann, T., Huang, R. J., and Kalberer, M.: Atmospheric analytical chemistry, Anal. Chem., 83, 4649-4664, 10.1021/ac2010718,
617   2011.
618 Huang, L., Coddens, E. M., and Grassian, V. H.: Formation of organosulfur compounds from aqueous phase reactions of S(IV) with
619   methacrolein and methyl vinyl ketone in the presence of transition metal ions, ACS Earth Space Chem., 3, 1749-1755,
620   10.1021/acsearthspacechem.9b00173, 2019.
621 Huang, L., Liu, T., and Grassian, V. H.: Radical-initiated formation of aromatic organosulfates and sulfonates in the aqueous phase,
622   Environ. Sci. Technol., 54, 11857-11864, 10.1021/acs.est.0c05644, 2020.
623 Huang, R.-J., Zhang, Y., Bozzetti, C., Ho, K.-F., Cao, J.-J., Han, Y., Daellenbach, K. R., Slowik, J. G., Platt, S. M., Canonaco, F.,
624   Zotter, P., Wolf, R., Pieber, S. M., Bruns, E. A., Crippa, M., Ciarelli, G., Piazzalunga, A., Schwikowski, M., Abbaszade, G.,
625   Schnelle-Kreis, J., Zimmermann, R., An, Z., Szidat, S., Baltensperger, U., El Haddad, I., and Prevot, A. S. H.: High secondary
626   aerosol contribution to particulate pollution during haze events in China, Nature, 514, 218-222, 10.1038/nature13774, 2014.
627 Huang, R.-J., Cao, J., Chen, Y., Yang, L., Shen, J., You, Q., Wang, K., Lin, C., Xu, W., Gao, B., Li, Y., Chen, Q., Hoffmann, T., amp,
628   apos, Dowd, C. D., Bilde, M., and Glasius, M.: Organosulfates in atmospheric aerosol: synthesis and quantitative analysis of
629      $PM_{2.5}$ from Xi'an, northwestern China, Atmos. Meas. Tech., 11, 3447-3456, 10.5194/amt-11-3447-2018, 2018.
630 Iinuma, Y., Mueller, C., Berndt, T., Boege, O., Claeys, M., and Herrmann, H.: Evidence for the existence of organosulfates from β-
631   pinene ozonolysis in ambient secondary organic aerosol, Environ. Sci. Technol., 41, 6678-6683, 2007a.
632 Iinuma, Y., Mueller, C., Boege, O., Gnauk, T., and Herrmann, H.: The formation of organic sulfate esters in the limonene ozonolysis
633   secondary organic aerosol (SOA) under acidic conditions, Atmos. Environ., 41, 5571-5583, 10.1016/j.atmosenv.2007.03.007,
634   2007b.
635 Iinuma, Y., Boege, O., Kahnt, A., and Herrmann, H.: Laboratory chamber studies on the formation of organosulfates from reactive
636   uptake of monoterpene oxides, Phys. Chem. Chem. Phys., 11, 7985-7997, 10.1039/b904025k, 2009.
637 Jiang, P.-Y., Katsumura, Y., Domae, M., Ishikawa, K., Ishigure, K., and Yoshida, Y.: Pulse radiolysis study of concentrated sulfuric
638   acid solutions. Formation mechanism, yield and reactivity of sulfate radicals, J. Chem. Soc., Faraday Trans., 88,
639   10.1039/ft9928801653, 1992.
640 Jimenez, J. L., Canagaratna, M. R., Donahue, N. M., Prevot, A. S. H., Zhang, Q., Kroll, J. H., DeCarlo, P. F., Allan, J. D., Coe, H.,
641   Ng, N. L., Aiken, A. C., Docherty, K. S., Ulbrich, I. M., Grieshop, A. P., Robinson, A. L., Duplissy, J., Smith, J. D., Wilson, K.
642   R., Lanz, V. A., Hueglin, C., Sun, Y. L., Tian, J., Laaksonen, A., Raatikainen, T., Rautiainen, J., Vaattovaara, P., Ehn, M., Kulmala,
643   M., Tomlinson, J. M., Collins, D. R., Cubison, M. J., Dunlea, E. J., Huffman, J. A., Onasch, T. B., Alfarra, M. R., Williams, P.
644   I., Bower, K., Kondo, Y., Schneider, J., Drewnick, F., Borrmann, S., Weimer, S., Demerjian, K., Salcedo, D., Cottrell, L., Griffin,
645   R., Takami, A., Miyoshi, T., Hatakeyama, S., Shimono, A., Sun, J. Y., Zhang, Y. M., Dzepina, K., Kimmel, J. R., Sueper, D.,
646   Jayne, J. T., Herndon, S. C., Trimborn, A. M., Williams, L. R., Wood, E. C., Middlebrook, A. M., Kolb, C. E., Baltensperger, U.,
647   and Worsnop, D. R.: Evolution of Organic Aerosols in the Atmosphere, Science, 326, 1525-1529, 10.1126/science.1180353,
648   2009.
649 Johnston, M. V. and Kerecman, D. E.: Molecular characterization of atmospheric organic aerosol by mass spectrometry, Annu. Rev.
650   Anal. Chem., 12, 247-274, 10.1146/annurev-anchem-061516-045135, 2019.
651 Kourtchev, I., Godoi, R. H. M., Connors, S., Levine, J. G., Archibald, A. T., Godoi, A. F. L., Paralovo, S. L., Barbosa, C. G. G.,
652   Souza, R. A. F., Manzi, A. O., Seco, R., Sjostedt, S., Park, J.-H., Guenther, A., Kim, S., Smith, J., Martin, S. T., and Kalberer,
653   M.: Molecular composition of organic aerosols in central Amazonia: an ultra-high-resolution mass spectrometry study, Atmos.
654   Chem. Phys., 16, 11899-11913, 10.5194/acp-16-11899-2016, 2016.
655 Kristensen, K. and Glasius, M.: Organosulfates and oxidation products from biogenic hydrocarbons in fine aerosols from a forest
656   in North West Europe during spring, Atmos. Environ., 45, 4546-4556, 10.1016/j.atmosenv.2011.05.063, 2011.
657 Kundu, S., Quraishi, T. A., Yu, G., Suarez, C., Keutsch, F. N., and Stone, E. A.: Evidence and quantitation of aromatic organosulfates
658   in ambient aerosols in Lahore, Pakistan, Atmos. Chem. Phys., 13, 4865-4875, 10.5194/acp-13-4865-2013, 2013.
659 Le Breton, M., Wang, Y., Hallquist, Å. M., Pathak, R. K., Zheng, J., Yang, Y., Shang, D., Glasius, M., Bannan, T. J., Liu, Q., Chan,
660   C. K., Percival, C. J., Zhu, W., Lou, S., Topping, D., Wang, Y., Yu, J., Lu, K., Guo, S., Hu, M., and Hallquist, M.: Online gas-
661   and particle-phase measurements of organosulfates, organosulfonates and nitrooxy organosulfates in Beijing utilizing a
662   FIGAERO ToF-CIMS, Atmos. Chem. Phys., 18, 10355-10371, 10.5194/acp-18-10355-2018, 2018.
663 Lewandowski, M., Jaoui, M., Offenberg, J. H., Krug, J. D., and Kleindienst, T. E.: Atmospheric oxidation of isoprene and 1,3-
664   butadiene: influence of aerosol acidity and relative humidity on secondary organic aerosol, Atmos. Chem. Phys., 15, 3773-3783,
665   10.5194/acp-15-3773-2015, 2015.
666 Liao, J., Froyd, K. D., Murphy, D. M., Keutsch, F. N., Yu, G., Wennberg, P. O., St. Clair, J. M., Crounse, J. D., Wisthaler, A.,
667   Mikoviny, T., Jimenez, J. L., Campuzano-Jost, P., Day, D. A., Hu, W., Ryerson, T. B., Pollack, I. B., Peischl, J., Anderson, B. E.,
668   Ziemba, L. D., Blake, D. R., Meinardi, S., and Diskin, G.: Airborne measurements of organosulfates over the continental US, J.
669   Geophys. Res.-Atmos., 120, 2990-3005, 10.1002/2014jd022378, 2015.

Lin, P., Yu, J. Z., Engling, G., and Kalberer, M.: Organosulfates in humic-like substance fraction isolated from aerosols at seven locations in East Asia: a study by ultra-high-resolution mass spectrometry, Environ. Sci. Technol., 46, 13118-13127, 10.1021/es303570v, 2012a.

Lin, Y. H., Zhang, Z., Docherty, K. S., Zhang, H., Budisulistiorini, S. H., Rubitschun, C. L., Shaw, S. L., Knipping, E. M., Edgerton, E. S., Kleindienst, T. E., Gold, A., and Surratt, J. D.: Isoprene epoxydiols as precursors to secondary organic aerosol formation: acid-catalyzed reactive uptake studies with authentic compounds, Environ. Sci. Technol., 46, 250-258, 10.1021/es202554c, 2012b.

Lin, Y. H., Zhang, H., Pye, H. O., Zhang, Z., Marth, W. J., Park, S., Arashiro, M., Cui, T., Budisulistiorini, S. H., Sexton, K. G., Vizuete, W., Xie, Y., Luecken, D. J., Piletic, I. R., Edney, E. O., Bartolotti, L. J., Gold, A., and Surratt, J. D.: Epoxide as a precursor to secondary organic aerosol formation from isoprene photooxidation in the presence of nitrogen oxides, P. Natl. Acad. Sci. USA, 110, 6718-6723, 10.1073/pnas.1221150110, 2013.

Liu, M. X., Song, Y., Zhou, T., Xu, Z. Y., Yan, C. Q., Zheng, M., Wu, Z. J., Hu, M., Wu, Y. S., and Zhu, T.: Fine particle pH during severe haze episodes in northern China, Geophys. Res. Lett., 44, 5213-5221, 10.1002/2017gl073210, 2017.

Liu, Y., and Wang, T.: Worsening urban ozone pollution in China from 2013 to 2017-Part 2: The effects of emission changes and implications for multi-pollutant control, Atmos. Chem. Phys., 20, 6323-6337, 10.5194/acp-20-6323-2020, 2020.

Lukacs, H., Gelencser, A., Hoffer, A., Kiss, G., Horvath, K., and Hartyani, Z.: Quantitative assessment of organosulfates in size-segregated rural fine aerosol, Atmos. Chem. Phys., 9, 231-238, 10.5194/acp-9-231-2009, 2009.

Ma, Y., Xu, X., Song, W., Geng, F., and Wang, L.: Seasonal and diurnal variations of particulate organosulfates in urban Shanghai, China, Atmos. Environ., 85, 152-160, 10.1016/j.atmosenv.2013.12.017, 2014.

Mahowald, N.: Aerosol indirect effect on biogeochemical cycles and climate, Science, 334, 794-796, 10.1126/science.1207374, 2011.

McNeill, V. F., Woo, J. L., Kim, D. D., Schwier, A. N., Wannell, N. J., Sumner, A. J., and Barakat, J. M.: Aqueous-phase secondary organic aerosol and organosulfate formation in atmospheric aerosols: a modeling study, Environ. Sci. Technol., 46, 8075-8081, 10.1021/es3002986, 2012.

Meade, L. E., Riva, M., Blomberg, M. Z., Brock, A. K., Qualters, E. M., Siejack, R. A., Ramakrishnan, K., Surratt, J. D., and Kautzman, K. E.: Seasonal variations of fine particulate organosulfates derived from biogenic and anthropogenic hydrocarbons in the mid-Atlantic United States, Atmos. Environ., 145, 405-414, 10.1016/j.atmosenv.2016.09.028, 2016.

Nah, T., Guo, H. Y., Sullivan, A. P., Chen, Y. L., Tanner, D. J., Nenes, A., Russell, A., Ng, N. L., Huey, L. G., and Weber, R. J.: Characterization of aerosol composition, aerosol acidity, and organic acid partitioning at an agriculturally intensive rural southeastern US site, Atmos. Chem. Phys., 18, 11471-11491, 10.5194/acp-18-11471-2018, 2018.

Nestorowicz, K., Jaoui, M., Rudzinski, K. J., Lewandowski, M., Kleindienst, T. E., Spolnik, G., Danikiewicz, W., and Szmigielski, R.: Chemical composition of isoprene SOA under acidic and non-acidic conditions: effect of relative humidity, Atmos. Chem. Phys., 18, 18101-18121, 10.5194/acp-18-18101-2018, 2018.

Nguyen, Q. T., Christensen, M. K., Cozzi, F., Zare, A., Hansen, A. M. K., Kristensen, K., Tulinius, T. E., Madsen, H. H., Christensen, J. H., Brandt, J., Massling, A., Nøjgaard, J. K., and Glasius, M.: Understanding the anthropogenic influence on formation of biogenic secondary organic aerosols in Denmark via analysis of organosulfates and related oxidation products, Atmos. Chem. Phys., 14, 8961-8981, 10.5194/acp-14-8961-2014, 2014.

Nguyen, T. B., Lee, P. B., Updyke, K. M., Bones, D. L., Laskin, J., Laskin, A., and Nizkorodov, S. A.: Formation of nitrogen- and sulfur-containing light-absorbing compounds accelerated by evaporation of water from secondary organic aerosols, J. Geophys. Res.-Atmos., 117, 10.1029/2011jd016944, 2012.

Nguyen, T. B., Bates, K. H., Crounse, J. D., Schwantes, R. H., Zhang, X., Kjaergaard, H. G., Surratt, J. D., Lin, P., Laskin, A., Seinfeld, J. H., and Wennberg, P. O.: Mechanism of the hydroxyl radical oxidation of methacryloyl peroxynitrate (MPAN) and its pathway toward secondary organic aerosol formation in the atmosphere, Phys. Chem. Chem. Phys., 17, 17914-17926, 10.1039/c5cp02001h, 2015.

Nozière, B., Kaberer, M., Claeys, M., Allan, J., D'Anna, B., Decesari, S., Finessi, E., Glasius, M., Grgic, I., Hamilton, J. F., Hoffmann, T., Iinuma, Y., Jaoui, M., Kahno, A., Kampf, C. J., Kourtchev, I., Maenhaut, W., Marsden, N., Saarikoski, S., Schnelle-Kreis, J., Surratt, J. D., Szidat, S., Szmigielski, R., and Wisthaler, A.: The molecular identification of organic compounds in the atmosphere: state of the art and challenges, Chem. Rev., 115, 3919-3983, 10.1021/cr5003485, 2015.

Nozière, B., Ekström, S., Alsberg, T., and Holmström, S.: Radical-initiated formation of organosulfates and surfactants in atmospheric aerosols, Geophys. Res. Lett., 37, 10.1029/2009gl041683, 2010.

Olson, C. N., Galloway, M. M., Yu, G., Hedman, C. J., Lockett, M. R., Yoon, T., Stone, E. A., Smith, L. M., and Keutsch, F. N.: Hydroxycarboxylic acid-derived organosulfates: synthesis, stability, and quantification in ambient aerosol, Environ. Sci. Technol., 45, 6468-6474, 10.1021/es201039p, 2011.

Olson, N. E., Lei, Z. Y., Craig, R. L., Zhang, Y., Chen, Y. Z., Lambe, A. T., Zhang, Z. F., Gold, A., Surratt, J. D., and Ault, A. P.: Reactive uptake of isoprene epoxydiols increases the viscosity of the core of phase-separated aerosol particles, ACS Earth Space Chem., 3, 1402-1414, 10.1021/acsearthspacechem.9b00138, 2019.

Passananti, M., Kong, L., Shang, J., Dupart, Y., Perrier, S., Chen, J., Donaldson, D. J., and George, C.: Organosulfate formation through the heterogeneous reaction of sulfur dioxide with unsaturated fatty acids and long-chain alkenes, Angew. Chem. Int. Ed. Engl., 55, 10336-10339, 10.1002/anie.201605266, 2016.

Pye, H. O. T., Pinder, R. W., Piletic, I. R., Xie, Y., Capps, S. L., Lin, Y. H., Surratt, J. D., Zhang, Z. F., Gold, A., Luecken, D. J., Hutzell, W. T., Jaoui, M., Offenberg, J. H., Kleindienst, T. E., Lewandowski, M., and Edney, E. O.: Epoxide pathways improve model predictions of isoprene markers and reveal key role of acidity in aerosol formation, Environ. Sci. Technol., 47, 11056-
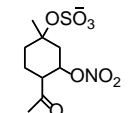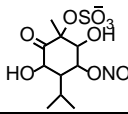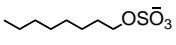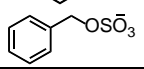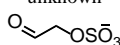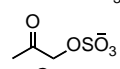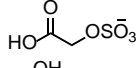
732   11064, 10.1021/es402106h, 2013.

733 Ramanathan, V., Crutzen, P. J., Lelieveld, J., Mitra, A. P., Althausen, D., Anderson, J., Andreae, M. O., Cantrell, W., Cass, G. R.,
734   Chung, C. E., Clarke, A. D., Coakley, J. A., Collins, W. D., Conant, W. C., Dulac, F., Heintzenberg, J., Heymsfield, A. J., Holben,
735   B., Howell, S., Hudson, J., Jayaraman, A., Kiehl, J. T., Krishnamurti, T. N., Lubin, D., McFarquhar, G., Novakov, T., Ogren, J.
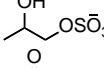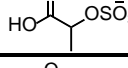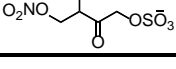736   A., Podgorny, I. A., Prather, K., Priestley, K., Prospero, J. M., Quinn, P. K., Rajeev, K., Rasch, P., Rupert, S., Sadourny, R.,
737   Satheesh, S. K., Shaw, G. E., Sheridan, P., and Valero, F. P. J.: Indian Ocean Experiment: an integrated analysis of the climate
738   forcing and effects of the great Indo-Asian haze, J. Geophys. Res.-Atmos., 106, 28371-28398, 10.1029/2001jd900133, 2001.

739 Rattanavaraha, W., Chu, K., Budisulistiorini, S. H., Riva, M., Lin, Y. H., Edgerton, E. S., Baumann, K., Shaw, S. L., Guo, H., King,
740   L., Weber, R. J., Neff, M. E., Stone, E. A., Offenberg, J. H., Zhang, Z., Gold, A., and Surratt, J. D.: Assessing the impact of
741   anthropogenic pollution on isoprene-derived secondary organic aerosol formation in PM$_{2.5}$ collected from the Birmingham,
742   Alabama, ground site during the 2013 Southern Oxidant and Aerosol Study, Atmos. Chem. Phys., 16, 4897-4914, 10.5194/acp-
743   16-4897-2016, 2017.

744 Riva, M., Tomaz, S., Cui, T., Lin, Y. H., Perraudin, E., Gold, A., Stone, E. A., Villenave, E., and Surratt, J. D.: Evidence for an
745   unrecognized secondary anthropogenic source of organosulfates and sulfonates: gas-phase oxidation of polycyclic aromatic
746   hydrocarbons in the presence of sulfate aerosol, Environ. Sci. Technol., 49, 6654-6664, 10.1021/acs.est.5b00836, 2015.

747 Riva, M., Budisulistiorini, S. H., Zhang, Z. F., Gold, A., and Surratt, J. D.: Chemical characterization of secondary organic aerosol
748   constituents from isoprene ozonolysis in the presence of acidic aerosol, Atmos. Environ., 130, 5-13,
749   10.1016/j.atmosenv.2015.06.027, 2016a.

750 Riva, M., Da Silva Barbosa, T., Lin, Y.-H., Stone, E. A., Gold, A., and Surratt, J. D.: Chemical characterization of organosulfates in
751   secondary organic aerosol derived from the photooxidation of alkanes, Atmos. Chem. Phys., 16, 11001-11018, 10.5194/acp-16-
752   11001-2016, 2016b.

753 Riva, M., Chen, Y., Zhang, Y., Lei, Z., Olson, N. E., Boyer, H. C., Narayan, S., Yee, L. D., Green, H. S., Cui, T., Zhang, Z., Baumann,
754   K., Fort, M., Edgerton, E., Budisulistiorini, S. H., Rose, C. A., Ribeiro, I. O., RL, E. O., Dos Santos, E. O., Machado, C. M. D.,
755   Szopa, S., Zhao, Y., Alves, E. G., de Sa, S. S., Hu, W., Knipping, E. M., Shaw, S. L., Duvoisin Junior, S., de Souza, R. A. F.,
756   Palm, B. B., Jimenez, J. L., Glasius, M., Goldstein, A. H., Pye, H. O. T., Gold, A., Turpin, B. J., Vizuete, W., Martin, S. T.,
757   Thornton, J. A., Dutcher, C. S., Ault, A. P., and Surratt, J. D.: Increasing Isoprene Epoxydiol-to-Inorganic Sulfate Aerosol Ratio
758   Results in Extensive Conversion of Inorganic Sulfate to Organosulfur Forms: Implications for Aerosol Physicochemical
759   Properties, Environ. Sci. Technol., 53, 8682-8694, 10.1021/acs.est.9b01019, 2019.

760 Schindelka, J., Iinuma, Y., Hoffmann, D., and Herrmann, H.: Sulfate radical-initiated formation of isoprene-derived organosulfates
761   in atmospheric aerosols, Faraday Discuss., 165, 237-259, 10.1039/c3fd00042g, 2013.

762 Shakya, K. M., and Peltier, R. E.: Investigating missing sources of sulfur at Fairbanks, Alaska, Environ. Sci. Technol., 47, 9332-
763   9338, 10.1021/es402020b, 2013.

764 Shakya, K. M., and Peltier, R. E.: Non-sulfate sulfur in fine aerosols across the United States: Insight for organosulfate prevalence,
765   Atmos. Environ., 100, 159-166, 10.1016/j.atmosenv.2014.10.058, 2015.

766 Shalamzari, M. S., Ryabtsova, O., Kahnt, A., Vermeylen, R., Herent, M. F., Quetin-Leclercq, J., Van der Veken, P., Maenhaut, W.,
767   and Claeys, M.: Mass spectrometric characterization of organosulfates related to secondary organic aerosol from isoprene, Rapid
768   Commun. Mass Spectrom., 27, 784-794, 10.1002/rcm.6511, 2013.

769 Shang, J., Passananti, M., Dupart, Y., Ciuraru, R., Tinel, L., Rossignol, S., Perrier, S., Zhu, T., and George, C.: SO$_2$ uptake on oleic
770   acid: a new formation pathway of organosulfur compounds in the atmosphere, Environ. Sci. Technol. Lett., 3, 67-72,
771   10.1021/acs.estlett.6b00006, 2016.

772 Shi, G. L., Xu, J., Peng, X., Xiao, Z. M., Chen, K., Tian, Y. Z., Guan, X. B., Feng, Y. C., Yu, H. F., Nenes, A., and Russell, A. G.:
773   aerosols in a polluted atmosphere: source contributions to highly acidic aerosol, Environ. Sci. Technol., 51, 4289-4296,
774   10.1021/acs.est.6b05736, 2017.

775 Shiraiwa, M., Ammann, M., Koop, T., and Poschl, U.: Gas uptake and chemical aging of semisolid organic aerosol particles, P. Natl.
776   Acad. Sci. USA, 108, 11003-11008, 10.1073/pnas.1103045108, 2011.

777 Shrivastava, M., Cappa, C. D., Fan, J. W., Goldstein, A. H., Guenther, A. B., Jimenez, J. L., Kuang, C., Laskin, A., Martin, S. T.,
778   Ng, N. L., Petaja, T., Pierce, J. R., Rasch, P. J., Roldin, P., Seinfeld, J. H., Shilling, J., Smith, J. N., Thornton, J. A., Volkamer,
779   R., Wang, J., Worsnop, D. R., Zaveri, R. A., Zelenyuk, A., and Zhang, Q.: Recent advances in understanding secondary organic
780   aerosol: Implications for global climate forcing, Rev. Geophys., 55, 509-559, 2017.

781 Song, S., Nenes, A., Gao, M., Zhang, Y., Liu, P., Shao, J., Ye, D., Xu, W., Lei, L., Sun, Y., Liu, B., Wang, S., and McElroy, M. B.:
782   Thermodynamic modeling suggests declines in water uptake and acidity of inorganic aerosols in Beijing winter haze events
783   during 2014/2015-2018/2019, Environ. Sci. Technol. Lett., 6, 752-760, 10.1021/acs.estlett.9b00621, 2019.

784 Staudt, S., Kundu, S., Lehmler, H. J., He, X., Cui, T., Lin, Y. H., Kristensen, K., Glasius, M., Zhang, X., Weber, R. J., Surratt, J. D.,
785   and Stone, E. A.: Aromatic organosulfates in atmospheric aerosols: synthesis, characterization, and abundance, Atmos. Environ.,
786   94, 366-373, 10.1016/j.atmosenv.2014.05.049, 2014.

787 Stone, E. A., Yang, L., Yu, L. E., and Rupakheti, M.: Characterization of organosulfates in atmospheric aerosols at Four Asian
788   locations, Atmos. Environ., 47, 323-329, 10.1016/j.atmosenv.2011.10.058, 2012.

789 Surratt, J. D., Kroll, J. H., Kleindienst, T. E., Edney, E. O., Claeys, M., Sorooshian, A., Ng, N. L., Offenberg, J. H., Lewandowski,
790   M., Jaoui, M., Flagan, R. C., and Seinfeld, J. H.: Evidence for organosulfates in secondary organic aerosol, Environ. Sci. Technol.,
791   41, 517-527, 10.1021/es062081q, 2007a.

792 Surratt, J. D., Lewandowski, M., Offenberg, J. H., Jaoui, M., Kleindienst, T. E., Edney, E. O., and Seinfeld, J. H.: Effect of acidity
793   on secondary organic aerosol formation from isoprene, Environ. Sci. Technol., 41, 5363-5369, 10.1021/es0704176, 2007b.

20

Surratt, J. D., Gómez-González, Y., Chan, A. W. H., Vermeylen, R., Shahgholi, M., Kleindienst, T. E., Edney, E. O., Offenberg, J. H., Lewandowski, M., Jaoui, M., Maenhaut, W., Claeys, M., Richard C. Flagan, and Seinfeld, J. H.: Organosulfate formation in biogenic secondary organic aerosol, J. Phys. Chem. A, 8345–8378, 2008.

Surratt, J. D., Chan, A. W., Eddingsaas, N. C., Chan, M., Loza, C. L., Kwan, A. J., Hersey, S. P., Flagan, R. C., Wennberg, P. O., and Seinfeld, J. H.: Reactive intermediates revealed in secondary organic aerosol formation from isoprene, P. Natl. Acad. Sci. USA, 107, 6640-6645, 10.1073/pnas.0911114107, 2010.

Tao, J., Zhang, L., Cao, J., and Zhang, R.: A review of current knowledge concerning $PM_{2.5}$ chemical composition, aerosol optical properties and their relationships across China, Atmos. Chem. Phys., 17, 9485-9518, 10.5194/acp-17-9485-2017, 2017.

Tao, S., Lu, X., Levac, N., Bateman, A. P., Nguyen, T. B., Bones, D. L., Nizkorodov, S. A., Laskin, J., Laskin, A., and Yang, X.: Molecular characterization of organosulfates in organic aerosols from Shanghai and Los Angeles urban areas by nanospray-desorption electrospray ionization high-resolution mass spectrometry, Environ. Sci. Technol., 48, 10993-11001, 10.1021/es5024674, 2014.

Tolocka, M. P., and Turpin, B.: Contribution of organosulfur compounds to organic aerosol mass, Environ. Sci. Technol., 46, 7978-7983, 10.1021/es300651v, 2012.

Wach, P., Spolnik, G., Rudzinski, K. J., Skotak, K., Claeys, M., Danikiewicz, W., and Szmigielski, R.: Radical oxidation of methyl vinyl ketone and methacrolein in aqueous droplets: characterization of organosulfates and atmospheric implications, Chemosphere, 214, 1-9, 10.1016/j.chemosphere.2018.09.026, 2019.

Wang, H. C., Chen, X. R., Lu, K. D., Hu, R. Z., Li, Z. Y., Wang, H. L., Ma, X. F., Yang, X. P., Chen, S. Y., Dong, H. B., Liu, Y., Fang, X., Zeng, L. M., Hu, M., and Zhang, Y. H.: NO_3 and N_2O_5 chemistry at a suburban site during the EXPLORE-YRD campaign in 2018, Atmos. Environ., 224, 10.1016/j.atmosenv.2019.117180, 2020a.

Wang, H. L., Qiao, L. P., Lou, S. R., Zhou, M., Ding, A. J., Huang, H. Y., Chen, J. M., Wang, Q., Tao, S. K., Chen, C. H., Li, L., and Huang, C.: Chemical composition of $PM_{2.5}$ and meteorological impact among three years in urban Shanghai, China, J. Clean Prod., 112, 1302-1311, 10.1016/j.jclepro.2015.04.099, 2016a.

Wang, J. J., Lu, X. M., Yan, Y. T., Zhou, L. G., and Ma, W. C.: Spatiotemporal characteristics of $PM_{2.5}$ concentration in the Yangtze River Delta urban agglomeration, China on the application of big data and wavelet analysis, Sci. Total Environ., 724, 10.1016/j.scitotenv.2020.138134, 2020b.

Wang, K., Zhang, Y., Huang, R. J., Wang, M., Ni, H., Kampf, C. J., Cheng, Y., Bilde, M., Glasius, M., and Hoffmann, T.: Molecular characterization and source identification of atmospheric particulate organosulfates using ultrahigh resolution mass spectrometry, Environ. Sci. Technol., 53, 6192-6202, 10.1021/acs.est.9b02628, 2019a.

Wang, S. Y., Zhou, S. M., Tao, Y., Tsui, W. G., Ye, J. H., Yu, J. Z., Murphy, J. G., McNeill, V. F., Abbatt, J. P. D., and Chan, A. W. H.: Organic peroxides and sulfur dioxide in aerosol: source of particulate sulfate, Environ. Sci. Technol., 53, 10695-10704, 10.1021/acs.est.9b02591, 2019b.

Wang, X. K., Rossignol, S., Ma, Y., Yao, L., Wang, M. Y., Chen, J. M., George, C., and Wang, L.: Molecular characterization of atmospheric particulate organosulfates in three megacities at the middle and lower reaches of the Yangtze River, Atmos. Chem. Phys., 16, 2285-2298, 10.5194/acp-16-2285-2016, 2016b.

Wang, Y., Ren, J., Huang, X. H. H., Tong, R., and Yu, J. Z.: Synthesis of four monoterpene-derived organosulfates and their quantification in atmospheric aerosol samples, Environ. Sci. Technol., 51, 6791-6801, 10.1021/acs.est.7b01179, 2017.

Wang, Y., Hu, M., Guo, S., Wang, Y., Zheng, J., Yang, Y., Zhu, W., Tang, R., Li, X., Liu, Y., Le Breton, M., Du, Z., Shang, D., Wu, Y., Wu, Z., Song, Y., Lou, S., Hallquist, M., and Yu, J.: The secondary formation of organosulfates under interactions between biogenic emissions and anthropogenic pollutants in summer in Beijing, Atmos. Chem. Phys., 18, 10693-10713, 10.5194/acp-18-10693-2018, 2018.

Wen, L., Xue, L. K., Wang, X. F., Xu, C. H., Chen, T. S., Yang, L. X., Wang, T., Zhang, Q. Z., and Wang, W. X.: Summertime fine particulate nitrate pollution in the North China Plain: increasing trends, formation mechanisms and implications for control policy, Atmos. Chem. Phys., 18, 11261-11275, 10.5194/acp-18-11261-2018, 2018.

Worton, D. R., Surratt, J. D., Lafranchi, B. W., Chan, A. W., Zhao, Y., Weber, R. J., Park, J. H., Gilman, J. B., de Gouw, J., Park, C., Schade, G., Beaver, M., Clair, J. M., Crounse, J., Wennberg, P., Wolfe, G. M., Harrold, S., Thornton, J. A., Farmer, D. K., Docherty, K. S., Cubison, M. J., Jimenez, J. L., Frossard, A. A., Russell, L. M., Kristensen, K., Glasius, M., Mao, J., Ren, X., Brune, W., Browne, E. C., Pusede, S. E., Cohen, R. C., Seinfeld, J. H., and Goldstein, A. H.: Observational insights into aerosol formation from isoprene, Environ. Sci. Technol., 47, 11403-11413, 10.1021/es4011064, 2013.

Yao, M., Zhao, Y., Hu, M., Huang, D., Wang, Y., Yu, J. Z., and Yan, N.: Multiphase reactions between secondary organic aerosol and sulfur dioxide: kinetics and contributions to sulfate formation and aerosol aging, Environ. Sci. Technol. Lett., 6, 768-774, 10.1021/acs.estlett.9b00657, 2019.

Yassine, M. M., Dabek-Zlotorzynska, E., Harir, M., and Schmitt-Kopplin, P.: Identification of weak and strong organic acids in atmospheric aerosols by capillary electrophoresis/mass spectrometry and ultra-high-resolution fourier transform ion cyclotron resonance mass spectrometry, Anal. Chem., 84, 6586-6594, 10.1021/ac300798g, 2012.

Zhang, H., Worton, D. R., Lewandowski, M., Ortega, J., Rubitschun, C. L., Park, J. H., Kristensen, K., Campuzano-Jost, P., Day, D. A., Jimenez, J. L., Jaoui, M., Offenberg, J. H., Kleindienst, T. E., Gilman, J., Kuster, W. C., de Gouw, J., Park, C., Schade, G. W., Frossard, A. A., Russell, L., Kaser, L., Jud, W., Hansel, A., Cappellin, L., Karl, T., Glasius, M., Guenther, A., Goldstein, A. H., Seinfeld, J. H., Gold, A., Kamens, R. M., and Surratt, J. D.: Organosulfates as tracers for secondary organic aerosol (SOA) formation from 2-methyl-3-buten-2-ol (MBO) in the atmosphere, Environ. Sci. Technol., 46, 9437-9446, 10.1021/es301648z, 2012.

Zhang, H., Zhang, Z., Cui, T., Lin, Y. H., Bhathela, N. A., Ortega, J., Worton, D. R., Goldstein, A. H., Guenther, A., Jimenez, J. L.,

856   Gold, A., and Surratt, J. D.: Secondary organic aerosol formation via 2-methyl-3-buten-2-ol photooxidation: evidence of acid-
857   catalyzed reactive uptake of epoxides, Environ. Sci. Technol. Lett., 1, 242-247, 10.1021/ez500055f, 2014.
858 Zheng, G., Su, H., Wang, S., Andreae, M. O., Poschl, U., and Cheng, Y.: Multiphase buffer theory explains contrasts in atmospheric
859   aerosol acidity, Science, 369, 1374-1377, 10.1126/science.aba3719, 2020.
860 Zhu, M., Jiang, B., Li, S., Yu, Q., Yu, X., Zhang, Y., Bi, X., Yu, J., George, C., Yu, Z., and Wang, X.: Organosulfur compounds
861   formed from heterogeneous reaction between SO2 and particulate-bound unsaturated fatty acids in ambient air, Environ. Sci.
862   Technol. Lett., 6, 318-322, 10.1021/acs.estlett.9b00218, 2019.
863
864

865 **Table 1.** Organosulfates (in ng m^{-3}) quantified by UPLC-ESI(-)-QToFMS.

Category	m/z, [M-H]$^-$	Formula, [M-H]$^-$	Retention time	Standards for quantification	Proposed structure	Ref.	Average concentration	
							2015/2016	2018/2019
Isoprene OS	167.0014	C$_4$H$_7$O$_5$S$^-$	0.85,1.36	Lactic acid sulfate (LAS)		a	1.13	1.45
	182.9963	C$_4$H$_7$O$_6$S$^-$	0.78,2.23	LAS		b	2.84	2.19
	197.0120	C$_5$H$_9$O$_6$S$^-$	0.85,1.55,3.11,3.99	LAS		c	1.87	1.72
	198.9912	C$_4$H$_7$O$_7$S$^-$	0.74,3.86	LAS		d	2.28	2.50
	199.0276	C$_5$H$_{11}$O$_6$S$^-$	0.85,8.08	LAS		c	0.57	0.65
	210.9912	C$_5$H$_7$O$_7$S$^-$	0.77	LAS		d	6.09	4.81
	213.0069	C$_5$H$_9$O$_7$S$^-$	0.84	LAS		d	3.81	3.82
	215.0226	C$_5$H$_{11}$O$_7$S$^-$	0.72	LAS		e	11.35	8.92
	237.0069	C$_7$H$_9$O$_7$S$^-$	0.87,1.5	LAS		f	0.58	0.50
	260.0076	C$_5$H$_{10}$NO$_9$S$^-$	1.19	LAS		g	2.28	2.96
	273.9869	C$_5$H$_8$NO$_{10}$S$^-$	1.3	LAS		h	1.89	4.87
Monoterpene OS	223.0276	C$_7$H$_{11}$O$_6$S$^-$	2.52,2.87,3.19,3.42	Glycolic acid sulfate (GAS)		i	1.37	1.12
	239.0225	C$_7$H$_{11}$O$_7$S$^-$	0.85,1.77,2.03,3.08	GAS		f	1.91	2.01
	249.0797	C$_{10}$H$_{17}$O$_5$S$^-$	5.34,5.60,6.85,7.04, 7.12,7.36	α-Pinene sulfate		j	0.33	0.17
	251.0589	C$_9$H$_{15}$O$_6$S$^-$	3.63,4.14,4.82,7.35	Limonaketone sulfate		j	1.32	1.02
	253.0382	C$_8$H$_{13}$O$_7$S$^-$	3.35,3.63,4.45	GAS		a	1.39	1.73
	279.0538	C$_{10}$H$_{15}$O$_7$S$^-$	3.42,4.34,4.55,4.71	GAS		g	2.99	4.00
	281.0695	C$_{10}$H$_{17}$O$_7$S$^-$	4.93,5.14	α-Pinene sulfate		f	0.34	0.21
	294.0648	C$_{10}$H$_{16}$NO$_7$S$^-$	8.14,9.02,9.16,9.35	α-Pinene sulfate		k	6.21	5.55

	m/z	Formula	Retention times	Name	Structure	Ref.	2015/2016	2018/2019
	296.0440	C9H14NO8S-	4.72,4.86,5.24,6.44	Limonaketone sulfate		k	1.62	2.29
	342.0495	C10H16NO10S-	4.57,4.71,5.17,7.35	Limonaketone sulfate		i	1.32	1.59
Anthropogenic OS	151.0065	C4H7O4S-	0.92,2.87,4.11,5.23, 5.39,8.21	Methyl sulfate	unknown	–	2.04	1.80
	194.9963	C5H7O6S-	0.82,2.86	GAS	unknown	–	0.83	0.76
	209.0120	C6H9O6S-	0.87,2.09,3.27,4.06	GAS	unknown	–	1.44	0.63
	209.0845	C8H17O4S-	9.64	Sodium octyl sulfate		–	1.04	0.86
	172.9909	C6H5O4S-	2.6	Phenyl sulfate		l	0.36	0.12
	187.0065	C7H7O4S-	4.54	Phenyl sulfate		l	0.35	0.17
C2/C3 OS	136.9909	C3H5O4S-	0.78,3.93	GAS	unknown	–	0.62	0.50
	138.9701	C2H3O5S-	0.69	GAS		g	0.58	0.57
	152.9858	C3H5O5S-	0.81	GAS		d	2.30	1.79
	154.9650	C2H3O6S-	0.69	GAS		m	2.91	2.25
	155.0014	C3H7O5S-	0.79	GAS		n	1.21	0.70
	168.9807	C3H5O6S-	0.82	LAS		m	2.24	1.94
Unknown source OS	164.9858	C4H5O5S-	0.79	Methyl sulfate		n	1.20	0.78
	241.9971	C5H8NO8S-	3.39,3.57,3.93,4.21	Methyl sulfate		n	1.67	1.21
SUM							**65.48**	**59.04**

866 *Retention times of each OS isomer considered in the quantification. References for proposed OS structures: [a] Schindelka et
867 al. (2013)), [b] Shalamzari et al. (2013), [c] Riva et al. (2016a), [d] Hettiyadura et al. (2015), [e] Surratt et al. (2010), [f] Nozière et al.
868 (2010), [g] (Surratt et al., 2007a) , [h] Nestorowicz et al. (2018), [i] Yassine et al. (2012), [j] Wang et al. (2017), [k] Surratt et al. (2008),
869 [l] Huang et al. (2018), [m] Olson et al. (2011), [n] Hettiyadura et al. (2019).

870

871

872

873 **Table 2.** A summary of OS concentration (in ng m^{-3}) and its contribution to OM (OS/OM) in four seasons in 2015/2016 and
874 2018/2019.

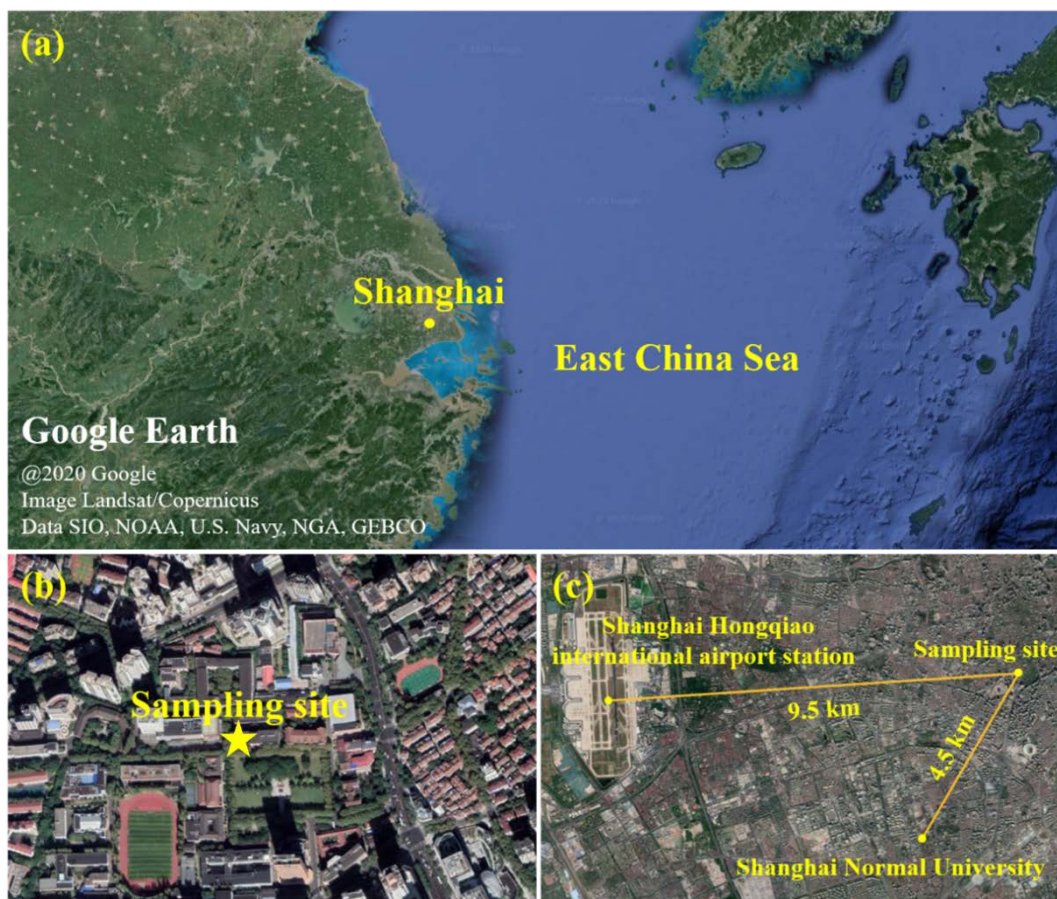| Season	2015/2016		2018/2019	
	OS	OS/OM	OS	OS/OM
All year	65.5±77.5	0.57%±0.56%	59.4±79.7	0.66%±0.56%
Spring	51.1±24.4	0.34%±0.10%	51.5±28.8	0.48%±0.15%
Summer	114.1±128.4	1.13%±0.78%	102.1±137.7	1.18%±0.81%
Autumn	38.2±21.7	0.36%±0.11%	38.0±20.0	0.54%±0.24%
Winter	44.5±17.5	0.32%±0.12%	37.3±18.4	0.36%±0.13%

875

876

877

Figure 1. (a) Map of Shanghai. **(b)** Map of the sampling site on the Xuhui Campus of Shanghai Jiao Tong University in downtown at 31.201°N, 121.429°E. **(c)** Map of the $PM_{2.5}$ sampling site, the meteorological station at Shanghai Hongqiao international airport, the air quality monitoring station at Shanghai Normal University, and distances between them.
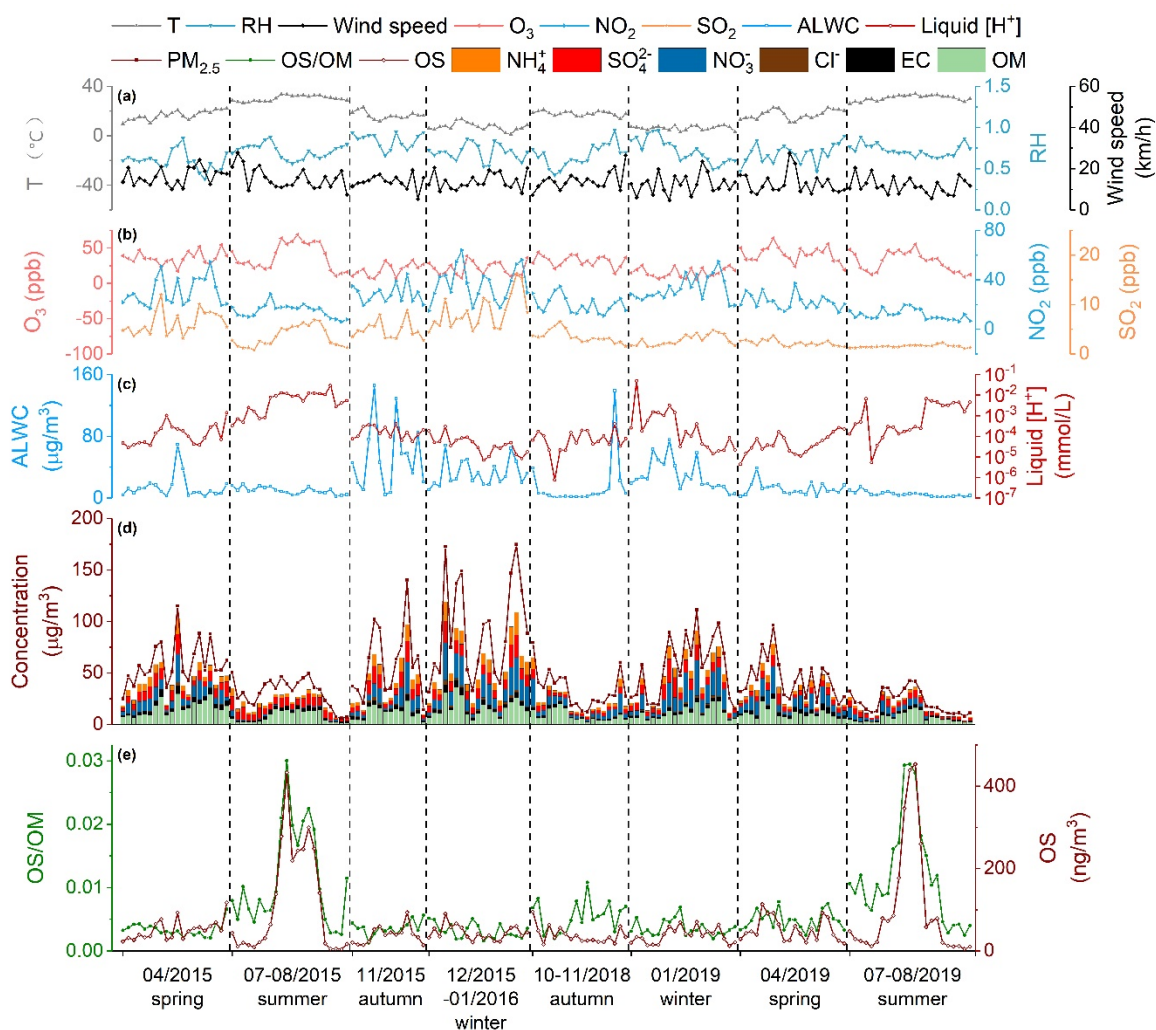
Figure 2. Time series of temperature, relative humid (RH), wind speed, O_3, NO_2, SO_2, aerosol liquid water content (ALWC) and liquid [H^+], concentrations of particulate organic matter (OM), elemental carbon (EC), sulfate, nitrate, chloride, ammonium, as well as the abundance of OS and its contribution to OM in 2015/2016 and 2018/2019 in Shanghai.
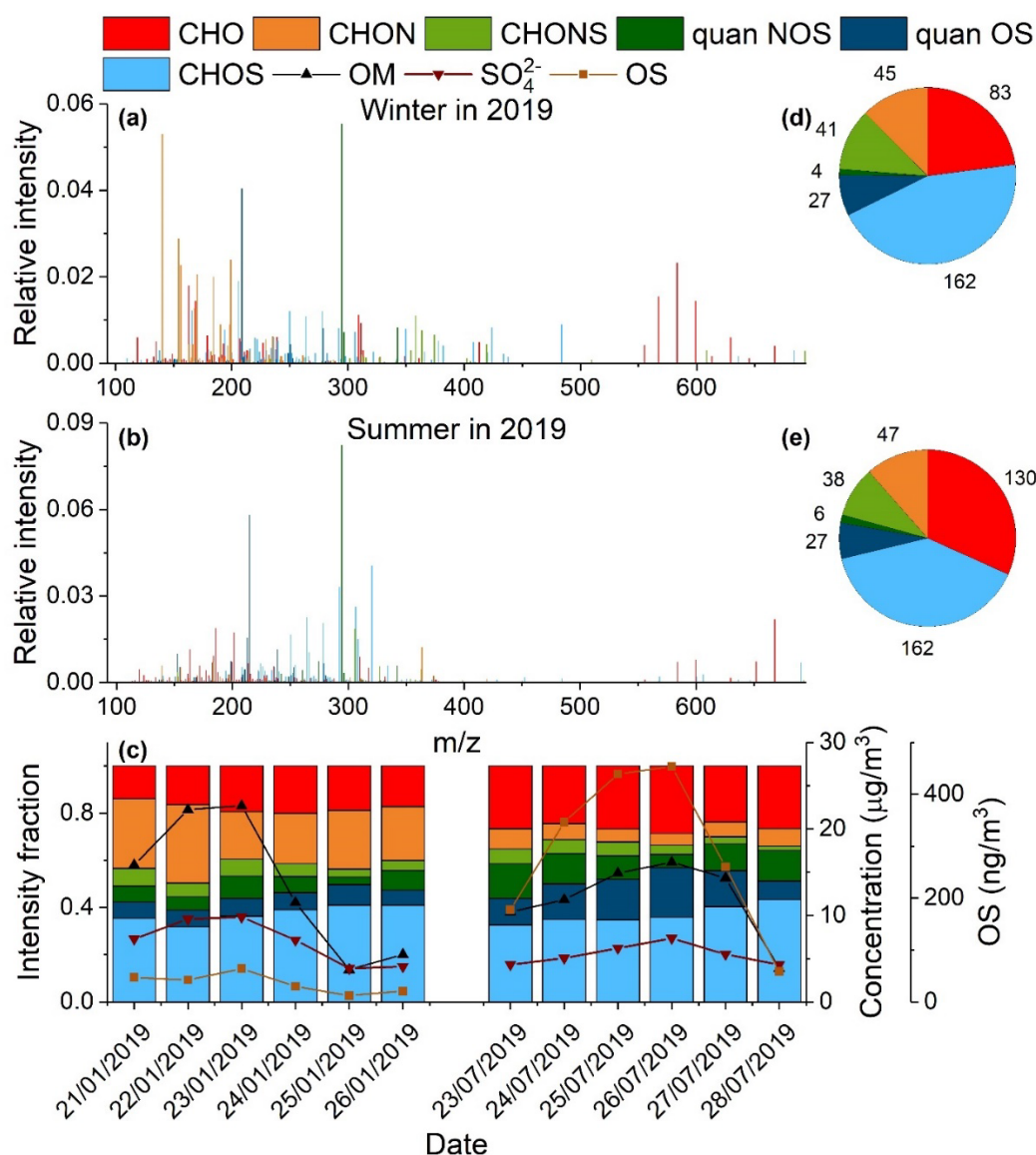
Figure 3. Average mass spectra of detected compounds in ambient aerosols during typical **(a)** wintertime (21-26 January 2019) and **(b)** summertime (23-28 July 2019) pollution episodes in Shanghai. The detected compounds were classified into six categories, i.e., CHO, CHON, CHOS, CHONS, quantified NOS, and quantified OS. The CHOS and CHONS categories excluded quantified OS and NOS, respectively. **(c)** The intensity fraction of different compound categories, as well as the time series of OM, SO_4^{2-}, and OS concentrations during two pollution episodes in 2019. **(d) (e)** The number of compounds detected in each category during the pollution episodes in winter and summer, respectively.
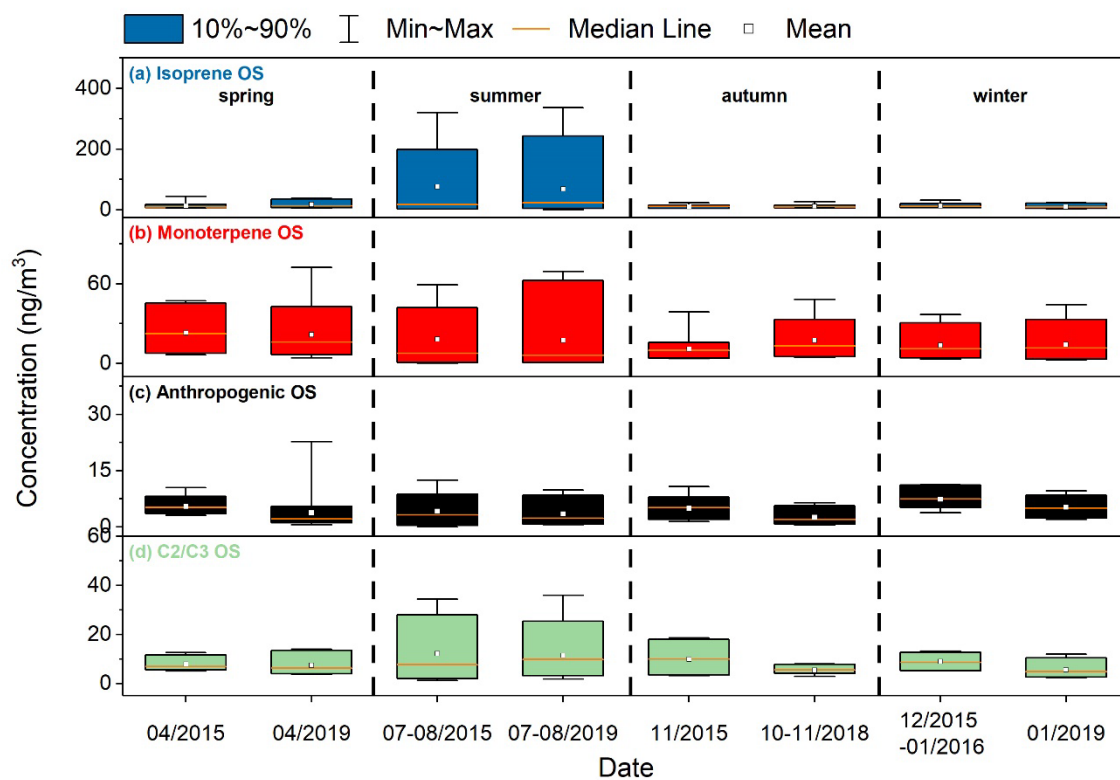
895

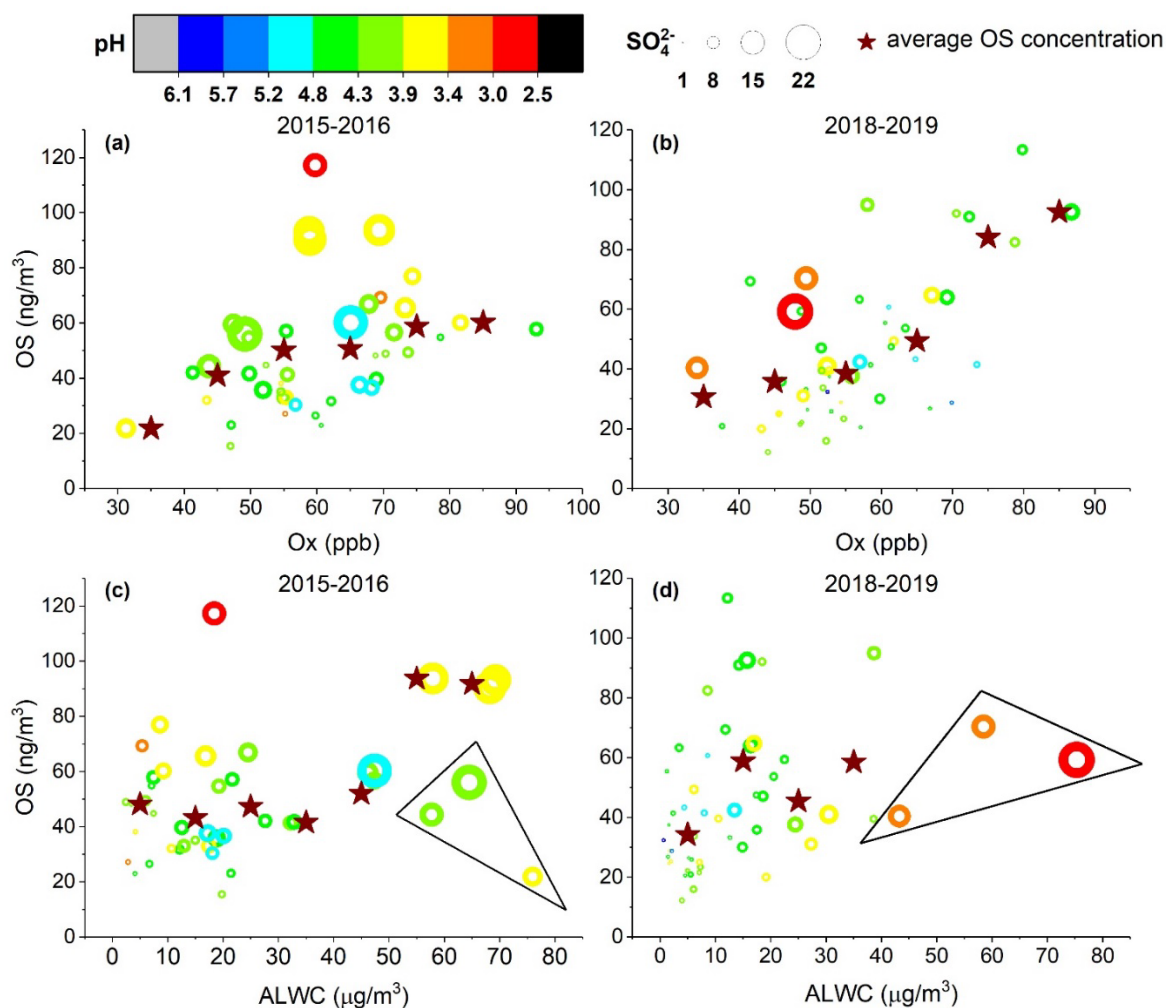896 **Figure 4.** The concentrations of different types of the quantified OS over four seasons in 2015/2016 and 2018/2019.

897

898

899 **Figure 5.** The quantified OS concentrations as a function of **(a) (b)** the level of O_x ($O_x = O_3 + NO_2$) and **(c)(d)** aerosol liquid

900 water content (ALWC) in 2015/2016 and 2018/2019 except for summer. The circles are colored according to the aerosol pH,

901 and their size is linearly scaled with the SO_4^{2-} concentration. The markers inside the triangle indicate the observations with

902 low O_x levels (<50 ppb). The measured OS concentrations within regular O_x or ALWC intervals (every ten unit-length) were

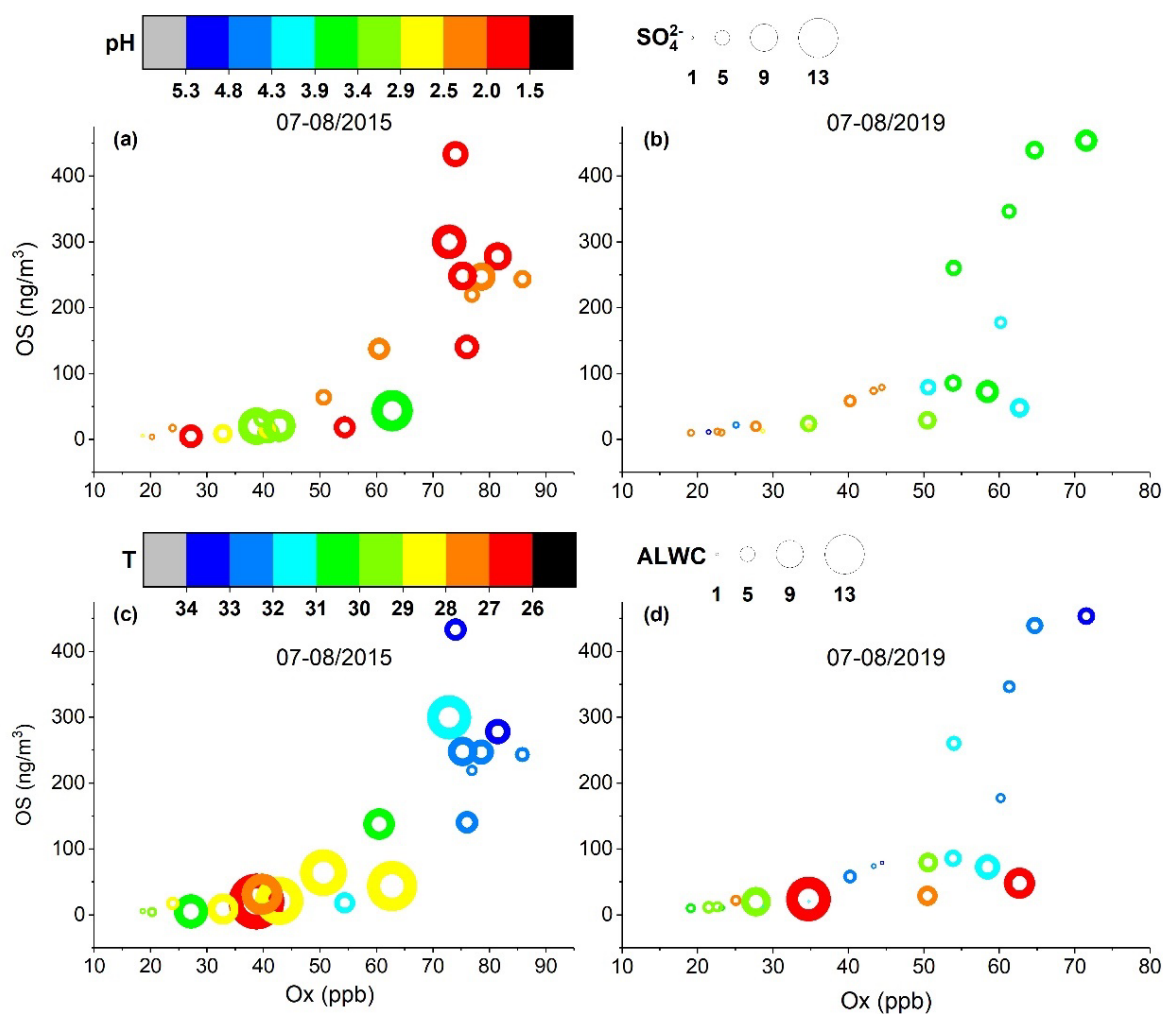903 averaged to more obviously demonstrate the trend (star symbols).

904

Figure 6. The quantified OS concentrations as a function of the Ox level in the summer of **(a) (c)** 2015 and **(b) (d)** 2019. The color of circles in **(a) (b)** indicates the aerosol pH, and their size is linearly scaled with the SO_4^{2-} concentration. The color of circles in **(c) (d)** indicates ambient temperature and their size is linearly scaled with aerosol liquid water content (ALWC).

908
909